Topological fluid mechanics of stirring

Philip L. Boyland[a], Hassan Aref[b] and Mark A. Stremler
Department of Theoretical and Applied Mechanics, University of Illinois, Urbana, IL 61801, USA

(Submitted to *Journal of Fluid Mechanics* –Thu, Apr 3, 1997)

A new approach to regular and chaotic fluid advection is presented that utilizes the topological concept of isotopy and the Thurston-Nielsen classification theorem. The prototypical problem of stirring by a finite number of stirrers of fluid confined to a disk is considered. The theory shows that for certain 'stirring protocols' a significant increase in complexity of the stirred motion – known as topological chaos – occurs when three or more stirrers are present and are moved about in particular ways. In this sense prior studies of chaotic advection with at most two stirrers, that were, furthermore, usually fixed in place and simply rotated about their axes, have been 'too simple.' We set out the basic theory without proofs and demonstrate the applicability of several topological concepts to fluid stirring. A key role is played by the representation of a given stirring protocol as a braid in a (2+1)-dimensional space-time made up of the flow plane and a time axis perpendicular to it. A simple experiment in which a viscous liquid is stirred by three stirrers has been conducted and is used to illustrate the theory.

1. Introduction

It is well known that even for laminar flow at very low Reynolds numbers stirring can lead to extremely complex flow patterns, and that the emergence of this complexity may be understood by an appeal to the theory of dynamical systems applied to the equations describing advection in the Lagrangian representation of that problem. This general phenomenon and topic is now known as *chaotic advection* (Aref 1984). Many studies over the past dozen years have shown the applicability of the notion of chaotic advection to flows of considerable importance for a variety of situations. For review and many examples see Ottino (1989, 1990) or Aref (1990, 1991, 1994).

Compared to earlier, often very empirical investigations the idea of chaotic advection represents a substantial step forward in our understanding of the nature of stirring of a fluid. The complexity of the resulting patterns is 'explained' by an appeal to chaos emerging in the advection equations, which for unsteady flow in two dimensions have the form

$$\frac{dx}{dt} = u(x,y,t) \;\; ; \;\; \frac{dy}{dt} = v(x,y,t), \tag{1.1}$$

where u and v are smooth functions of their arguments. The system (1.1) is rich enough to have chaotic solutions even for flow fields of very simple functional form. However, the reliance on specific forms of the velocity field (u,v), although appealing from an applications point of view and helpful in establishing a link between theory and experiment, tends to hide even more basic mathematical structures. Clearly, stirring and mixing of a fluid depend on basic topological properties of the fluid region being stirred. Indeed, it will become apparent that the *metric* details of u and v sometimes do not matter much, but the *topological* nature of the flow-field that they represent is crucial. The main purpose of this paper is to elaborate on this statement.

The topological approach adopted here looks at a very general level of structure, eliminates

a) Permanent address: Department of Mathematics, University of Florida, Gainesville, FL 32601, USA.
b) To whom correspondence should be addressed.

many specifics of the problem, but retains enough information to draw conclusions that have wide applicability, and that therefore classify different flows into 'universality classes.' This general insight has already led workers in fluid mechanics to study topological approaches to the subject in many other contexts (see, for example, the proceedings edited by Moffatt & Tsinober 1990, or the general audience article by Ricca & Berger 1996). The term 'topological fluid mechanics' has been used for this emerging disciplinary area.

Imagine a domain in the plane filled with fluid. By some stirring action – which we shall specify in a moment – this fluid domain is mapped onto itself. We wish to explore the consequences of the most basic assumptions regarding this mapping, which in the fluid mechanics literature are usually made without much comment. Thus, in keeping with the generally accepted basis for a continuum fluid description, the mapping instant by instant is differentiable, one-to-one, and its inverse is differentiable, i.e., it is a *diffeomorphism.* We shall also assume that area is preserved, corresponding to an incompressible fluid, although most of our results hold without that assumption. For a viscous fluid we insist that every point at the boundary of the fluid region moves with the (solid) boundary that delimits it. To consider an inviscid fluid, we would allow slip along the boundary. In either case it is well known that one can prove the existence of a fixed point, i.e., the existence of a fluid particle that has not moved between the initial and final configurations, in the interior of the domain. The simplest variant of this result is known as Brouwer's fixed point theorem. For most readers, unfamiliar with recent developments in the theory of dynamical systems using topological methods, this is presumably thought to be as far as topological considerations can take one in the problem of fluid stirring (and does not appear to be a result of great practical importance). A key point of this paper, which evolved from a series of discussions between a mathematician (PLB) versed in the theory of topological chaos in dynamical systems, and two fluid mechanicians interested in fluid stirring and mixing, is that much more interesting and far-reaching results are available.

An overview of this work was presented at the 49th Annual Meeting of the American Physical Society, Division of Fluid Dynamics in Syracuse, NY (Boyland, Aref & Stremler 1996; Aref, Boyland & Stremler 1996).

2. Isotopy to the identity

Consider the prototypical case of fluid inside a circular disk, D, with a number, k, of identical, movable, cylindrical stirrers inserted as indicated in Fig.2.1. The choice of a disk shape or the shape of the cross-section of any agitator is entirely irrelevant, of course, but for ease of visualization we consider all boundaries to be circular. We assume that the configuration is always of the kind indicated in Fig.2.1 – we are not interested in singularities associated with the collision of stirrers or of stirrers hitting the boundary. The region occupied by fluid in the initial state is designated R_k, where the subscript reminds us of how many stirrers ('holes') there are in the fluid region. The general stirring action consists of a motion of one or more stirrers along specified trajectories within the disk such that at the end of a 'stirring cycle' the set of stirrers are at the same positions as when the cycle began (although generally permuted, and possibly rotated about their axes). We are also going to allow the outer boundary to rotate during the stirring cycle. The prescribed motion of stirrers and external boundary is called the *stirring protocol.*[1] Again for

1) The term "stirring protocol" was used in a similar sense by Aref & Balachandar (1986), although in that study the geometry of the fluid region was fixed and the "stirring protocol" consisted simply in a prescription of how and when to rotate the two eccentric cylinders doing the stirring and between which the fluid was situated.

simplicity let the fluid be very viscous, so that we may assume it only moves when the stirrers move, and that it comes to rest immediately when the stirrers stop. It will be clear from the nature of our arguments that they can be extended to other physical situations as well, but this case is the simplest to consider.

During the motion of the stirrers each fluid particle moves from an initial position to a final position. However, in general, instant by instant the region occupied by fluid changes due to the motion of the stirrers, i.e., the diffeomorphism is not from R_k to R_k (although the domain and range of the diffeomorphism are topologically equivalent – each a disk with k holes). At the end of the cycle the fluid again occupies the original region R_k. We call the diffeomorphism of R_k onto R_k produced by one such stirring cycle the *stirred motion.*

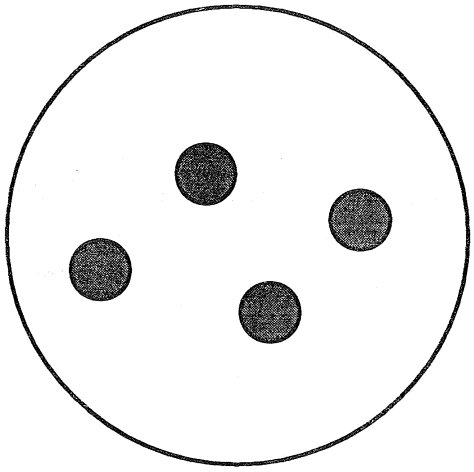

Figure 2.1: Generic 'batch' stirring device considered – a disk of fluid with k embedded stirrers.

There is a particularly simple class of diffeomorphisms corresponding to those cases in which the stirrers simply rotate about their axes while remaining in fixed positions and in which we also allow the outer boundary to rotate. For these diffeomorphisms the fluid region is R_k for all time, not just at the end of each stirring cycle. In fact, most studies of chaotic advection in Stokes flow to date have employed diffeomorphisms of precisely this type (cf. Aref & Balachandar 1986; Chaiken, Chevray, Tabor & Tan 1986; Jana, Metcalfe & Ottino 1994). We call these diffeomorphisms *fixed stirrer motions.* A fixed stirrer motion is a one-parameter family of diffeomorphisms, with time t as the parameter. We shall designate such a family by a Greek lowercase letter with time as a subscript, e.g., ψ_t. For t=0, i.e., before any stirrer or the disk boundary has moved, we clearly have $\psi_0 = \mathbf{id}$, the identity.

In the topological theory the fixed stirrer motions are augmented substantially by considering the class of all diffeomorphisms that map R_k onto itself while keeping the stirrers at fixed positions (and only allowing them and the outer boundary to rotate). In the terminology of mechanics we may think of this expanded class of diffeomorphisms as *virtual motions,* each of which might be produced by an externally imposed, distributed force-field acting on the fluid while the stirring takes place. The augmented class of diffeomorphisms is a very large collection of mappings indeed. We shall call all of them the *fixed stirrer diffeomorphisms.* (It is even possible to relax the constraint of incompressibility and enlarge the class of fixed stirrer diffeomorphisms further to include compressible flows, but this will not be necessary in our discussion.) Every fixed stirrer

motion is, of course, a fixed stirrer diffeomorphism, but the latter class contains many more mappings. It will become apparent shortly why it is important to work with the larger class of mappings even though it contains many elements with a somewhat artificial fluid-mechanical interpretation.

Let h: $R_k \to R_k$ be a stirred motion corresponding to some stirring protocol involving k stirrers. One says that h is *isotopic to the identity* if there exists a parametrized set of fixed stirrer diffeomorphisms, ψ_τ, $0 \le \tau \le 1$, such that $\psi_0 = \mathrm{id}$ and $\psi_1 = h$. Thus, if h is isotopic to the identity, the same net result concerning the stirring of the fluid by moving the k stirrers about could have been obtained by a fixed stirrer diffeomorphism. From a fluid mechanics standpoint we might have been content to write the definition of isotopy in terms of fixed stirrer motions. The definition given is clearly much more demanding: the class of mappings in the definition is huge compared to the actual possible motions accessible by rotating the stirrers about fixed positions and rotating the outer boundary. The main point of interest, however, is the topological result that *for $k \ge 3$ there exist stirred motions that are not isotopic to the identity.* Such stirred motions would *a fortiori* not be isotopic to the identity using the restricted class of fixed stirrer motions. In other words, for $k \ge 3$ there are stirred motions that are not equivalent to motions with a fixed geometry (up to in-place rotations) even if all possible force distributions for moving particles around are allowed!

It is obvious that for k=0 (no internal stirrers) the stirred motion h is isotopic to the identity. For if h corresponds to a rotation of the disk boundary by some angle α, the family of fixed stirrer diffeomorphisms can simply be chosen such that ψ_τ corresponds to rotation by an angle $\tau\alpha$.

Already the case of a single stirrer, k=1, is more challenging. Is h isotopic to the identity in this case? Let us consider a particular version of the problem of stirring by a single stirrer in which the stirrer moves on a circular trajectory, concentric with the disk. In this case fixed stirrer diffeomorphisms can be found in the following way: Consider the flow from a frame of reference that moves with the stirrer maintaining its axes parallel to the axes in the fixed 'laboratory' frame with which the moving frame coincides at t=0. In this moving frame the geometry of disk and stirrer is fixed, except for possible rotations in place of either or both boundaries. Hence, the fixed stirrer diffeomorphisms produced by rotating the stirrer and disk boundaries in accord with the circular orbit of the stirrer augmented by the overall rotation of the stirrer will produce the stirring in the 'laboratory' frame that the moving stirrer does. In particular, this family of fixed stirrer diffeomorphisms shows that h is isotopic to the identity.

It is from stirred motions that are not isotopic to the identity that one expects to see 'topological chaos'. Intuitively speaking, these stirred motions 'tangle up' the fluid so badly that the process cannot be replicated (or, equivalently, undone) within a very broad class of mappings when the configuration of stirrers is held fixed. More precisely, we use the term 'topological chaos' in the following sense: Topology is the study of properties that are unchanged under continuous deformations. Thus, topological chaos refers to dynamical complexity that cannot be removed by continuous deformations of the shape of the fluid region, the precise trajectories of stirrers (given their starting and ending points and the way in which they loop around one another) and so on (see also §4.1).

Basic topological theorems state that for k = 0 or 1 any stirred motion is isotopic to the identity. For k = 2 either the stirred motion itself or its second iterate is isotopic to the identity (see Birman

1975). To find a stirred motion that is not isotopic to the identity we must, therefore, have at least three stirrers. Recalling the literature on chaotic advection (see the references given in the Introduction), we thus see that in this sense all the configurations investigated to date have been 'too simple.' It has been possible to produce chaos, of course, as has been verified many times, but the richer topological chaos that can be achieved with three (or more) stirrers has not been 'built in' to the setup (although it may arise 'accidentally' – see §7). We shall elucidate this new regime of topologically chaotic, stirred motion and provide examples of its appearance.

The remainder of the paper is set out as follows. In §3 we develop some of the topological tools necessary to discuss the notion of *isotopy of diffeomorphisms* and the deformations of material lines in a fluid. Just as a stirred motion can be isotopic to the identity, two stirred motions can be isotopic to one another, and the stirred motion in question will fall into one of a set of classes known as *isotopy classes.* In §4 we give a synopsis of the results available in *Thurston-Nielsen theory*, which describes the stirred motions in terms of their isotopy classes and classifies them into three basic types. In particular, there is a type with very complicated motions known as *pseudo-Anosov* (pA) mappings. These mappings are related to the well-known *cat map,* and are characterized by exponential stretching and contraction everywhere governed by stretching rates, λ and λ^{-1}, that may be calculated. Other quantitative results, such as the existence of an infinite number of periodic orbits, where the number of orbits of a given periodicity may be counted, may also be deduced for pA maps. These complicated dynamics are present in every isotopic map.

In §5 we show how the chosen stirring protocol can be associated with a *braid* in a (2+1) - dimensional 'space-time' obtained by augmenting the plane in which the stirring takes place with a time-axis. We define what is known as *the braid group* and explain its physical significance and how it can parametrize isotopy classes. The braid group on three strands has a representation in terms of 2×2 matrices with integer entries, and this representation leads to an algorithm for calculating the stretching rate, λ, as an eigenvalue of the appropriate matrix.

Thurston-Nielsen theory has been applied to the problem of driven oscillators by McRobie & Thompson (1993), and the reader may find their treatment a useful supplement to ours. MacKay (1990) has speculated on the importance of Thurston-Nielsen theory to steady 3D flows.

In §6 we focus on k = 3, the simplest case to yield topological chaos, and provide further details from the general theory outlined in the preceding sections for this particular case. We also show results of a physical experiment that illustrates the applicability of the theory to viscous mixing. Our concluding §7 contains discussion and mentions various extensions that may be productive for future work. The Appendix contains mathematical details on the connection of torus maps to stirred motions for k=3.

3. Isotopic diffeomorphisms

In this section we introduce various topological definitions and tools that are required to analyze the diffeomorphisms called stirred motions in §2 (for general background see Seifert & Threlfall 1980; Birman 1975). First, we consider the notion of *isotopic diffeomorphisms.* In §2 we defined isotopy to the identity. Heuristically, two diffeomorphisms are said to be isotopic if one can be deformed continuously into the other. Formally, two diffeomorphisms f and g from R_k to R_k are said to be *isotopic* if there is another diffeomorphism, h, that is isotopic to the identity (see §2), such that $g = hf$, i.e., g is the result of first operating with f, then with h.

Thinking in terms of fluid stirring in R_k, two stirred motions f and g are isotopic if we can accomplish the same stirred motion as g by first performing the stirred motion dictated by f and then follow it by a fixed stirrer diffeomorphism h. Given a stirred motion (or, in general, any diffeomorphism), f, all diffeomorphisms that are isotopic to f are called its *isotopy class.* The fixed stirrer diffeomorphisms introduced in §2 are then simply the class of diffeomorphisms isotopic to the identity.

The notion of *isotopic curves* is closely related. By a *simple loop* in R_k we mean a closed curve that has no self-intersections. More precisely, a simple loop Γ is a continuous, one-to-one map from the circle, S^1, into R_k. Two simple loops, Γ_1 and Γ_2, are said to be isotopic if one can be continuously deformed into the other through a family of simple loops. Isotopy of simple arcs with their ends on the boundary of the fluid region is defined similarly. Note that in this case the isotopy allows the ends of the arc to slip along the boundary (corresponding either to inviscid boundary conditions, or to rotation of the components of the boundary for viscous flow).

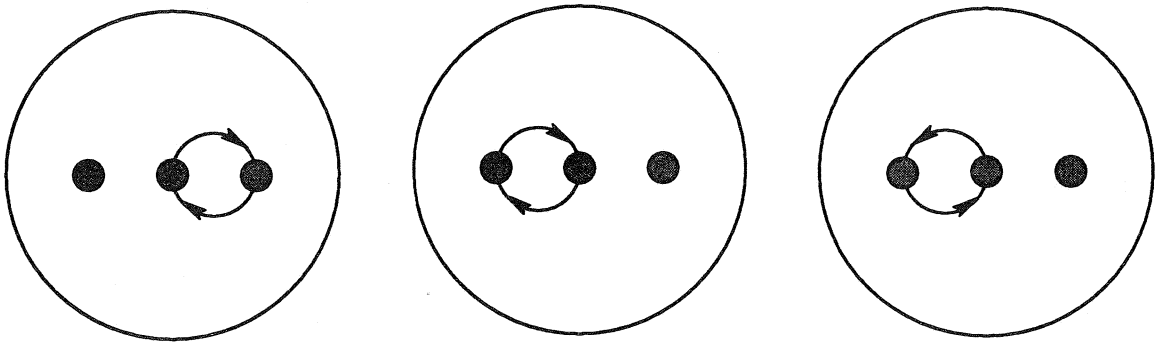

Figure 3.1: Illustration of stirred motions: (a) R_+; (b) L_+; (c) L_-.

One can show that Γ_1 and Γ_2 are isotopic if and only if there exists a diffeomorphism, h, isotopic to the identity, such that $h(\Gamma_1) = \Gamma_2$. In particular, if a given diffeomorphism, h, is isotopic to the identity, then for any simple loop, Γ, the image of Γ under h must be isotopic to Γ.

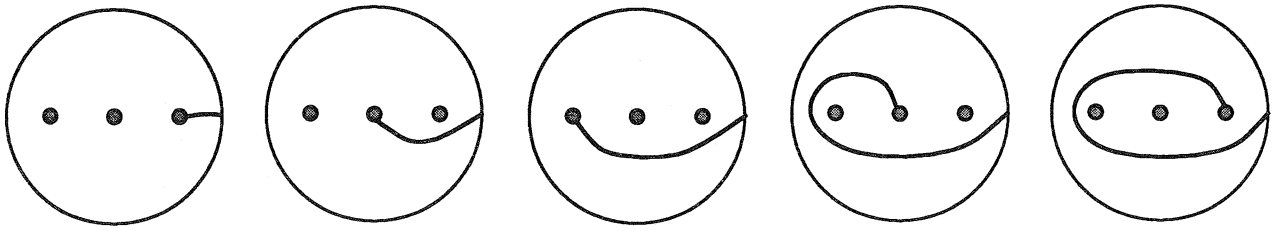

Figure 3.2: Illustration of finite order stirred motion:
(a) Initial position of Γ; (b) $R_+(\Gamma)$; (c) $f(\Gamma)$; (d) $f^2(\Gamma)$; (e) $f^3(\Gamma)$

Using the ideas just introduced we now consider two example stirred motions of R_3 onto itself, one of which has its third iterate isotopic to the identity, whereas the other does not. Referring to Fig.3.1(a) let R_+ denote the stirred motion produced by rotating the middle and right stirrer about the midpoint of the line joining them through 180° in a clockwise sense. Similarly, let L_+ denote the stirred motion produced by rotating the middle and left stirrer about the midpoint of the line joining them through 180° in a clockwise sense (Fig.3.1(b)). If, instead, we rotate by 180° in the

counterclockwise sense, we designate the stirred motion L_- (Fig.3.1(c)). We now consider the two stirred motions that arise by following R_+ by L_+ and L_-, respectively, i.e., $f = L_+ R_+$, and $g = L_- R_+$. From an engineering point of view, e.g., from the magnitude of forces acting on the stirrers or from the energetics of the motion, the two motions f and g are indistinguishable. Topological considerations, however, reveal a profound difference between these two ways of effecting the stirring of the fluid.

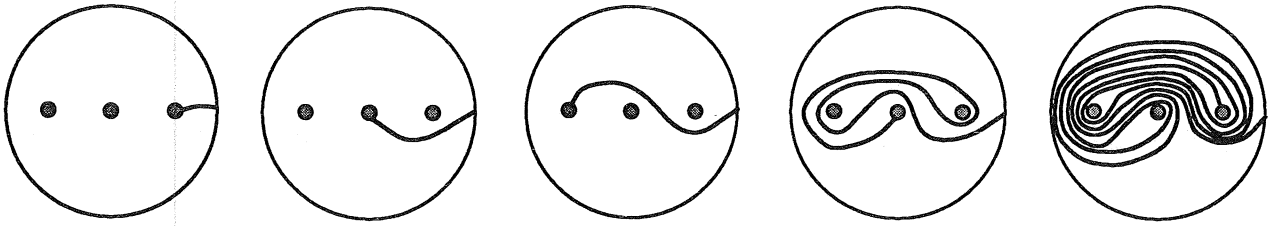

Figure 3.3: Illustration of pseudo-Anosov stirred motion:
(a) Initial position of Γ; (b) $R_+(\Gamma)$; (c) $g(\Gamma)$; (d) $g^2(\Gamma)$; (e) $g^3(\Gamma)$

Consider the material line, Γ, a simple arc, initially connecting the right stirrer to the boundary, as shown in Figs.3.2(a) and 3.3(a). Using only the continuity of the fluid motion we see that under R_+ the line Γ is deformed as indicated in Figs.3.2(b) and 3.3(b). We do not know, of course, exactly where the line $R_+(\Gamma)$ will be. This depends on details of the dynamics governing the fluid motion. However, this line must clearly still connect the boundary and the stirrer, and because of the motion being clockwise it must somehow pass 'below' the right position – more precisely, it must be isotopic to what is shown in the figure. Application of the stirred motions L_+ and L_-, respectively, to produce $f(\Gamma)$ and $g(\Gamma)$, now yields the results shown in Figs.3.2(c) and 3.3(c). The difference is readily apparent: No continuous fluid motion holding the stirrers fixed (i.e., a fixed stirrer motion) can deform the material line in Fig. 3.2(c) to that in Fig.3.3(c). Thus, f is not isotopic to g. If we continue the iterations, the difference becomes ever more dramatic. Figures 3.2(e) and 3.3(e) show the results (up to isotopy) of 3 iterates. At this point each stirrer has returned to its initial position. By rotating the outer boundary the arc in Fig.3.2(e) can be deformed back to its initial position, shown in Fig.3.2(a), and, indeed, f^3 is isotopic to the identity. Figure 3.3(e) indicates that this clearly is not the case for g^3.

4. Thurston-Nielsen theory

It turns out that, in fact, most stirred motions are not isotopic to the identity. Thurston-Nielsen theory (Thurston 1988[2]; Fathi, Lauderbach & Poenaru 1979; Casson & Bleiler 1988; Handel 1985; for a review of dynamical systems applications see Boyland, 1994; for a general audience write-up of the mathematical contributions of Jakob Nielsen see Lundsgaard-Hansen, 1993) describes and categorizes these transformations in terms of their isotopy classes. The classification theorem stated below says that within each isotopy class there exists a special diffeomorphism, called the *Thurston-Nielsen (TN) representative,* which is in a precise topological and dynamical sense the simplest map in the isotopy class. Once the properties of the TN representative are understood, we know what dynamical and topological complexity must be present in every

2) This paper was widely circulated as a preprint in 1975.

diffeomorphism of the isotopy class in question. This result conveys the power of the theory. It will be described in greater detail below and illustrated by a physical experiment.

4.1 *The Thurston-Nielsen representative*

We give first a precise statement of the

Thurston-Nielsen classification theorem: *If f is a homeomorphism of a compact surface, S, then f is isotopic to a homeomorphism, φ, of one of the following types:*

(i) *Finite order:* $\varphi^n = \mathrm{id}$ *for some integer* $n>0$;

(ii) *Pseudo-Anosov:* φ *preserves a pair of transverse, measured foliations,* $\mathcal{F}_u$ *and* $\mathcal{F}_s$, *and there is a* $\lambda > 1$ *such that* φ *stretches* $\mathcal{F}_u$ *by a factor* λ *and contracts* $\mathcal{F}_s$ *by* λ^{-1};

(iii) *Reducible:* φ *fixes a family of reducing curves, and on the complementary surfaces* φ *satisfies* (i) *or* (ii).

Note that the theorem applies to the more general class of homeomorphisms (invertible, continuous maps) while we have focussed here on diffeomorphisms since these arise naturally as stirred motions.

We see, then, that the TN representative, φ, is of one of three basic types. The *finite order* homeomorphisms are very simple dynamically. They have the property that the TN representative composed with itself a certain number of times is the identity. For the fixed stirrer diffeomorphisms of R_k one can show that the only finite order homeomorphism is the identity. Hence, the TN representative for the isotopy class containing the identity is the identity itself. The finite order homeomorphisms arising from a cyclic permutation of the three stirrers are all rigid rotations about the center of the disk (in the appropriate coordinates).

The second type of TN representative, the *pseudo-Anosov (pA) homeomorphisms,* are dynamically very complicated. We shall discuss them in greater detail in the next subsection. The cat map on the torus is an example of a (pseudo-)Anosov map. In particular, the measured foliations in the theorem statement are the collections of all the stable and unstable manifolds of all points in S, and the last phrase in (ii) reflects that there is stretching and contraction everywhere by the factors λ and λ^{-1}, respectively (see §4.2). The presence of a pA homeomorphism in an isotopy class has strong implications for the dynamics and stirring produced by all mappings in the class as indicated by

Handel's isotopy stability theorem: *If* φ *is pseudo-Anosov and* f *is isotopic to* φ, *then there is a compact,* f*-invariant set,* Y, *and a continuous, onto* $\alpha : Y \to S$, *that is homotopic to the inclusion, so that* $\alpha f = \varphi \alpha$.

This theorem makes precise the sense in which the dynamics of the pA map φ are present in the dynamics of any isotopic map f. The set Y contains the 'memory' of the pA dynamics, because for any $x \in S$ there is $y \in Y$ with $\alpha(y) = x$. Since $\alpha f = \varphi \alpha$, $\alpha(f^n(y)) = \varphi^n(\alpha(y))$ for all n. Thus, α sends the orbit of y under f to that of x under φ, and so every orbit of the pA map φ is reflected

in some orbit of f contained in Y. (If the pA orbit is periodic, the f-orbit can be chosen to be periodic.) This clarifies the meaning of the term 'topological chaos'. The dynamics of the pA map remains after continuous deformation, i.e., under isotopy. Note that the set Y is perhaps not all of S, and the map α may be many-to-one. This allows the dynamics of f to be more complicated than those of φ; but the dynamics of f can never be less complicated.

The third type of TN representative is called *reducible,* since in this case there is a collection of disjoint, simple loops (the 'reducing curves' in the classification theorem) with the property that they are permuted by the TN representative. Cutting along these loops, we obtain a collection of smaller domains, and on each of these the TN representative is either finite order or pA.

A given isotopy class will only contain a TN representative of one type. Thus, we can call the isotopy class itself finite order, pseudo-Anosov or reducible depending on what kind of TN-representative it contains. An important question, then, is how does one tell to what type of isotopy class a given stirred motion belongs? And, after this is ascertained, what implications does the nature of the TN representative have for the dynamics and mixing properties of the stirred motion itself? There is an algorithm due to Bestvina and Handel (1995; see also Franks & Misiurewicz 1993; Los 1993) that answers both of these questions. There is a computer implementation of it, but the algorithm is quite complicated and we are content here to discuss cases that are of relevance to stirred motions with three stirrers.

4.2 *Anosov and pseudo-Anosov maps*

Pseudo-Anosov maps or homeomorphisms are a generalization of the more familiar Anosov mappings. We first briefly outline the theory of linear Anosov diffeomorphisms on the two-dimensional torus T^2. This theory provides a convenient way to understand the properties of pseudo-Anosov maps that are of importance here. In addition, the linear Anosov maps on T^2 will be seen to be closely connected with the pseudo-Anosov maps on R_3 (see Appendix). For more detailed information on linear Anosov maps, Markov partitions and invariant foliations, see Devaney (1989), Robinson (1995) or Katok & Hasselblatt (1995).

To obtain a linear Anosov map on T^2, one starts with a positive integer matrix,

$$\mathbf{M} = \begin{pmatrix} a & b \\ c & d \end{pmatrix}, \tag{4.2}$$

with unit determinant, $ad - bc = 1$, and $a + d > 2$. The matrix $\mathbf{M}$ induces a mapping, $f_{\mathbf{M}}$, on the plane via $f_{\mathbf{M}}(x,y) = (ax + by, cx + dy)$. Since this map preserves the integer lattice, it can be used to induce a map, $\phi_{\mathbf{M}}$, on the two-torus T^2 (thought of as a square with opposite sides identified). Perhaps the simplest such matrix is

$$\mathbf{M} = \begin{pmatrix} 2 & 1 \\ 1 & 1 \end{pmatrix}. \tag{4.3}$$

In this case $\phi_{\mathbf{M}}$ is often called *Thom's toral automorphism* or the *cat map* after a well known figure in the book by Arnol'd and Avez (1968).

The conditions on the matrix $\mathbf{M}$ insure that it has two distinct eigenvalues $\lambda > 1$ and $1/\lambda$. The

eigendirection corresponding to λ is called the *unstable direction;* the other eigendirection is called the *stable direction.* Since the Jacobian matrix of ϕ_M at every point is M, the map uniformly stretches by λ in the unstable direction and contracts by $1/\lambda$ in the stable direction. All the unstable directions (i.e., all the unstable manifolds of points) fit together into what is called the *unstable foliation.* This structure is invariant under the action of ϕ_M. The conditions on M imply that its eigenvectors have irrational slope. Thus, the unstable foliation is a wrapping of the torus by lines with irrational slope. The *stable foliation* is defined analogously.

An Anosov diffeomorphism always gives rise to a *Markov partition* that allows one to code the orbits using symbolic dynamics. For a linear Anosov mapping, ϕ_M, the Markov partition can be chosen so that its *transition matrix* is M. The trace of M^n counts the number of fixed points of $(\phi_M)^n$, and so the number of periodic orbits of order n of ϕ_M grows as λ^n.

Perhaps less well known are the topological aspects of the linear Anosov diffeomorphisms on the two-torus. Simple loops on T^2 can be represented by pairs of relatively prime integers. The pair (p,q) can be thought of as the arc in the plane that connects the origin to the point (p,q), or else this arc pushed down to the torus, which yields a loop that wraps p times around one direction of the torus and q times around the other. The image of the loop under ϕ_M is just the loop represented by M acting on (p,q). Its n'th iterate is $M^n\begin{pmatrix}p\\q\end{pmatrix}$, and so the lengths of loops grow like powers of the largest eigenvalue of M, namely λ^n. Using a similar argument, one sees that the asymptotic direction of iterated loops is controlled by the unstable eigendirection. Thus, under iteration, all loops converge to the unstable foliation of ϕ_M. Similar remarks hold for the behavior of sets (i.e., 'patches' of advected fluid) under iteration.

Even less known is the fact that these basic properties of Anosov maps persist under isotopy (see Franks, 1970). More precisely, if g is isotopic to ϕ_M, then the lengths of loops grow under iteration of g at least at the rate of λ^n. Further, the periodic points of ϕ_M are present (in the appropriate sense) in g, so the number of fixed points of g^n grows at least at the rate of λ^n. Finally, under iteration by g, loops and patches eventually converge (in a precise topological sense) to the unstable foliation of ϕ_M.

Pseudo-Anosov homeomorphisms are quite similar to linear Anosov maps with one essential difference. The unstable foliation of a linear Anosov map can be seen as defining a non-vanishing vector field on the two-torus. Such vector fields cannot exist on other surfaces (except the annulus). Thus, for example, no diffeomorphism of the fluid region R_k can have an unstable foliation that defines a vector field that is non-vanishing everywhere. However, the region R_k can have a homeomorphism of pseudo-Anosov type. In pseudo-Anosov maps there is still uniform stretching and contraction at each point by a stretch factor λ. The unstable and stable directions still fit together into invariant unstable and stable foliations, but these foliations must have a finite number of points (called singularities or prongs) where there are three or more stable directions and the same number of unstable directions. Additional singular behavior is also allowed on the boundary.

Despite the presence of these singularities, a pseudo-Anosov map, ϕ, shares most of the basic properties of Anosov maps. There is a Markov partition with transition matrix M that allows one

to code the dynamics of ϕ, and the largest eigenvalue of M is the stretching factor $\lambda>1$. The number of fixed points of ϕ^n grows like λ^n as does the length of non-trivial loops under iteration. In addition, the iterated loops converge to the unstable foliations. Finally, these properties are shared by any diffeomorphism that is isotopic to ϕ (by Handel's theorem, §4.1).

From the perspective of fluid stirring pseudo-Anosov diffeomorphisms are especially attractive. They give area-preserving maps of the region with uniform stretching and contraction at each point. Thus, there are no elliptic islands in which material becomes trapped away from the rest of the fluid impeding mixing. In fact, this property (when stated a bit more precisely) uniquely characterizes the pA map in an isotopy class (up to a change of coordinates). Unfortunately, we do not at this time know how to realize an actual pA map by a motion of the stirrers in a realistic fluid model. However, we can identify many pA isotopy classes and, as noted above, the complexity of the pA map in the class provides a lower bound for the complexity of any element in its isotopy class. Hence, we may conclude that stirred motions with three or more stirrers, as discussed here and realized experimentally in §6, can have very complicated dynamical and topological behavior.

5. Braids and isotopy classes

Braids specify isotopy classes on a region R_k. (For general information on braids, see Birman 1975). In essence, the braid provides a graphical representation of the stirring protocol in the space-time made up of the two-dimensional fluid disk and a time-axis perpendicular to it (and oriented upward). The algebraic description of braids will allow us to label stirred motions and their isotopy classes.

We first define a *physical braid on n strands.* Pick n points, P_1, P_2,..., P_n in the disk D. Place two copies of D in a (2+1)-dimensional space-time, one directly above the other. The first, 'earlier' copy of the disk, D_0, is on the plane $\tau = 0$; the second, 'later' copy, D_1, on the plane $\tau = 1$. A physical braid, b, is a collection of n non-intersecting arcs (or strands) that connect the points P_i on D_0 to the points P_i on D_1 (see Fig.5.1). Each distinguished point in the first disk is connected to exactly one distinguished point in the second disk. For simplicity we always assume that the strands move upward (in the direction of increasing time, τ) without 'vertical back-tracking.' The braid is intended to keep track of how the stirrers are permuted during one cycle of the stirred motion.

Artin's braid group, B_n, gives an algebraic description of the physical braids on n strands. The generators of this group are the simple braids σ_i, i=1,...,n, that interchange the i'th and (i+1)'st strands, and their inverses σ_i^{-1}. We choose to let σ_i denote an interchange of stirrers i and i+1 such that these 'orbit' one another in a clockwise sense. Thus, if the three stirrers considered in Figs.3.1-3.3, or in Fig.5.1, are labelled 1, 2, 3 from left to right, the stirred motion R_+ would be represented by the braid σ_2 (the first interchange of two strands in Fig.5.1(a) or (b)). The stirred motions L_+ and L_- would be represented by σ_1 and σ_1^{-1}, respectively (see the second interchange of strands in Fig.5.1(a), (b), respectively). The composition of two generators, $\sigma_i\sigma_j$, represents the braid obtained by putting the braid σ_i 'after' (i.e., in the sense of Fig.5.1 'on top of') σ_j. Thus, in our earlier example in §3, the braid corresponding to f is $\sigma_1\sigma_2$, whereas the braid corresponding to g is $\sigma_1^{-1}\sigma_2$.

Since one wants physical braids that can be continuously deformed into one another to have the

same algebraic description, one needs to add certain relations to the definition of the group, namely $\sigma_i\sigma_{i+1}\sigma_i = \sigma_{i+1}\sigma_i\sigma_{i+1}$, and for $|i-j| \geq 2$, $\sigma_i\sigma_j = \sigma_j\sigma_i$ (see Birman, 1975, figure p.8).

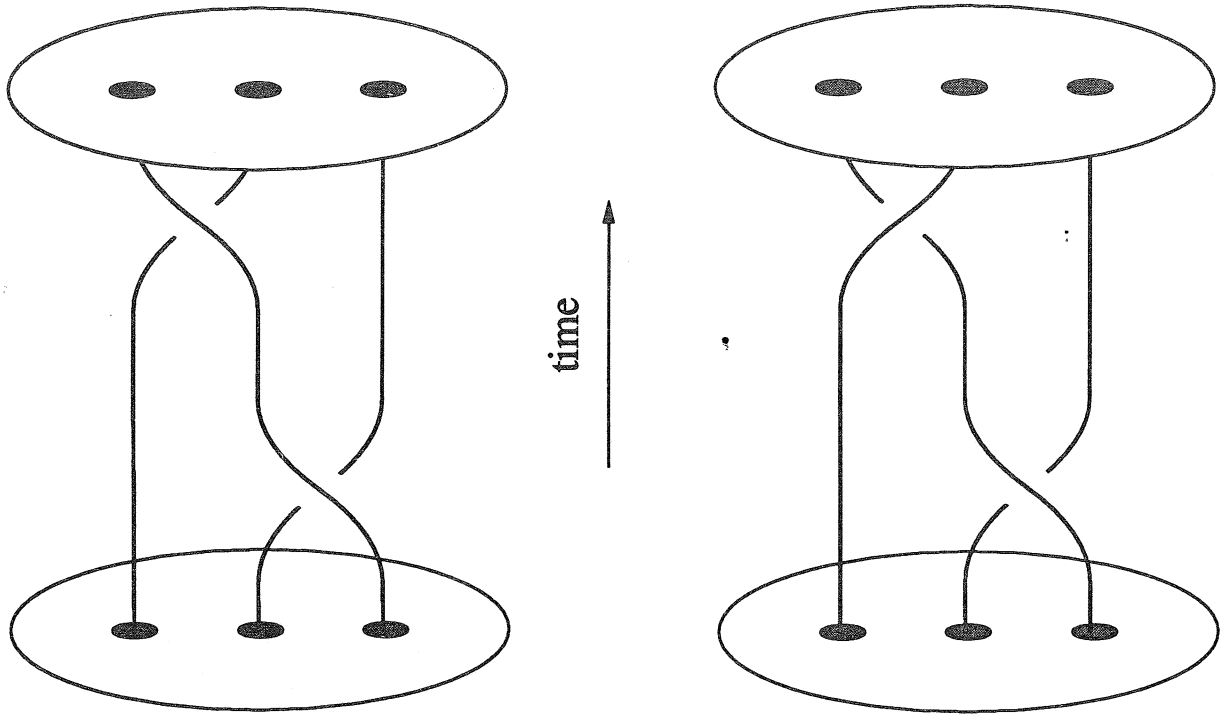

Figure 5.1: Stirred motions as braids in (2+1)-dimensional space-time, here for three strands. (a) Finite order stirring protocol; (b) pseudo-Anosov stirring protocol.

An element of the braid group will be called a *mathematical braid* to distinguish it from a physical braid. Each physical braid can be assigned a mathematical braid by projecting it onto a given plane perpendicular to the flow-plane and keeping track of over- and under-crossings. Changing the projection plane can clearly change the resulting braid. It is not too difficult to see that the resulting change is always conjugation in the group B_n, i.e., if the original braid is β, the braid in the new projection will be of the form $\alpha\beta\alpha^{-1}$, where the braid α reflects the change of coordinates from the old projection plane to the new one. It is also the case that if one physical braid can be deformed into another (without breaking the strands), then the two physical braids are assigned the same mathematical braid.

The braid group has many uses, but the application of importance here is its role as a device for labeling stirred motions of a region R_k and their isotopy classes. From the intuitive picture given of the correspondence between stirring protocols and physical braids (cf. Fig.5.1) it is clear that each stirring protocol corresponds to a braid, and to each braid there corresponds a stirring protocol.

We saw in §2 that a stirring protocol with k stirrers gives rise to a diffeomorphism of R_k. We have just seen that such a stirring protocol also yields a physical braid and thus a mathematical braid. Now we need to connect the isotopy classes of the stirred motions to mathematical braids. There is almost a unique correspondence, but since we have allowed rotation along the boundaries of R_k in defining isotopy, we must be a bit careful in stating this correspondence. For example, the stirred motion on three strands represented by $(\sigma_1\sigma_2)^3$ is isotopic to the identity because it can

be 'undone' by rotating the outer boundary once. The correct statement is that two stirring protocols with k stirrers yield isotopic diffeomorphisms if (and only if) their mathematical braids are equal up to multiplication by some number of full twists of the outer boundary of R_k. In algebraic language the precise statement is that the elements of the braid group are equal in B_k modulo the subgroup generated by $(\sigma_1\sigma_2...\sigma_{k-1})^k$.

Intuitively, this last result is seen to be true as follows: Consider two stirring protocols and the physical braids they generate. If these can be deformed into one another, it implies, on one hand, that they have the same mathematical braid and, on the other hand, that the three-dimensional deformation that takes one physical braid to the other can be used to generate a family of two-dimensional diffeomorphisms that carry out the isotopy of one stirred motion to the other. In more mathematical terms, the proof proceeds by showing that the set of isotopy classes is a group with multiplication as the rule of composition. This group is then shown to be isomorphic to the quotient of B_k discussed above by showing that the isotopy class group is generated by classes that switch two stirrers, i.e., by the classes that correspond to the elements σ_i.

6 The case k = 3

The case k=3 is the first for which Thurston-Nielsen theory allows the existence of a stirred motion isotopic to a pA diffeomorphism. We expect such motions to stir the fluid particularly well. Fortunately, for this case virtually all aspects of the Thurston-Nielsen theory can be computed explicitly and fairly easily using a connection with torus maps. We have already indicated how stirring protocols for the region R_3 lead to physical braids, and how these braids label isotopy classes. It turns out that on the two-torus each isotopy class of diffeomorphisms contains exactly one linear Anosov map, ϕ_M (isotopy of diffeomorphisms on the torus is defined analogously to that on the regions R_k), of the kind discussed in §4.2. In Thurston-Nielsen theory, this linear Anosov map is the TN representative in its class. This particular diffeomorphism, then, is represented by a certain matrix with integer entries, and its properties can be calculated from this matrix. The correspondence between torus maps and diffeomorphisms on R_3 preserves the matrix. Hence, each stirred motion on R_3 is represented by a certain 2×2 matrix with integer entries, which yields properties of the TN representative for the isotopy class to which the stirred motion belongs. There are a number of technical details to be considered, in particular how to map the torus onto R_3, that we have collected in the Appendix. Here we proceed directly and more heuristically to a representation of the braid group on three strands by 2×2 matrices with integer entries.

6.1 Matrix representations of braids

Consider the set of three stirrer positions and the two material lines connecting them as shown in Fig.6.1(a). Under the stirred motion corresponding to σ_2 the stirrers and material lines are transformed into Fig.6.1(b) (modulo deformations that can be accomplished with fixed stirrers). Hence, since the line I is mapped to I′, which 'is like' I and II of the original configuration, and since II is mapped to II′, i.e., in essence to itself, we can represent σ_2 by the matrix

$$\mathbf{M}_2 = \begin{pmatrix} 1 & 0 \\ 1 & 1 \end{pmatrix}. \tag{6.1}$$

We may view the assignment of 0 and 1 to the entries in this matrix in the spirit of an 'incidence matrix' as used in circuit theory: The rows correspond to the original material lines I and II, and the columns to their transformed versions I′ and II′. Since I′ 'consists of' I and II, we have placed 1s in both entries of the first column; similarly, since II′ is just II, in the second column we have placed a 0 in the first row and a 1 in the second row. Another interpretation comes from treating I and II as boxes in a Markov partition.

Analogously, the matrix representing σ_1^{-1} is taken as (see Fig.6.2)

$$\mathbf{M}_1^{-1} = \begin{pmatrix} 1 & 1 \\ 0 & 1 \end{pmatrix} \tag{6.2}$$

We construct the matrices corresponding to other simple braids by invoking the group properties of the braid group to which this representation should be faithful. In particular, the matrix corresponding to σ_1 is

$$\mathbf{M}_1 = \begin{pmatrix} 1 & 1 \\ 0 & 1 \end{pmatrix}^{-1} = \begin{pmatrix} 1 & -1 \\ 0 & 1 \end{pmatrix}. \tag{6.3}$$

Fig.6.1: Transformation of the two lines, I and II, connecting the stirrers under R_+.
(a) Initial position of I and II; (b) Position of transformed segments I′ and II′ up to deformation.

Thus, if, as in §§3 and 5, we consider the stirred motion f corresponding to the braid $\sigma_1\sigma_2$, we find that its matrix representation is

$$\mathbf{M}_f = \mathbf{M}_1\mathbf{M}_2 = \begin{pmatrix} 1 & -1 \\ 0 & 1 \end{pmatrix}\begin{pmatrix} 1 & 0 \\ 1 & 1 \end{pmatrix} = \begin{pmatrix} 0 & -1 \\ 1 & 1 \end{pmatrix}. \tag{6.4}$$

This matrix has the property $\mathbf{M}_f^3 = -\mathbf{1}$, where $\mathbf{1}$ is the 2×2 unit matrix. Hence, $\mathbf{M}_f^6$ is the identity, in accord with the finite order nature of f.

Fig.6.2: Transformation of the two lines, I and II, connecting the stirrers under L_-.
(a) Initial position of I and II; (b) Position of transformed segments I′ and II′ up to deformation.

On the other hand, the matrix representation of the braid $\sigma_1^{-1}\sigma_2$, which corresponds to the stirred motion g from §§3 and 5, is

$$\mathbf{M}_g = \mathbf{M}_1^{-1}\mathbf{M}_2 = \begin{pmatrix} 1 & 1 \\ 0 & 1 \end{pmatrix}\begin{pmatrix} 1 & 0 \\ 1 & 1 \end{pmatrix} = \begin{pmatrix} 2 & 1 \\ 1 & 1 \end{pmatrix}, \tag{6.5}$$

i.e., precisely the matrix that appears in the cat map, which has eigenvalues $\frac{1}{2}(3 \pm \sqrt{5})$.

TN theory shows that the stirred motion 'inherits' a number of features from the underlying linear map represented by the matrix $\mathbf{M}_g$ (see Appendix). Thus, the isotopy class containing the stirred motion g stretches 'topologically essential' material lines by a factor $\frac{1}{2}(3+\sqrt{5})$ on each iteration, and the number of periodic points of period n of g is bounded below by $\mathrm{Tr}(\mathbf{M}_g^n)$. We conclude[3] that g has at least three fixed points; that at least seven points are fixed under g^2 – the three fixed points are included here, so there are two different period-two *orbits*; at least 18 points are fixed under g^3 (so there are five different period-three *orbits*); at least 15,127 points are fixed under g^{10}, and so on. For large n, $\mathrm{Tr}(\mathbf{M}_g^n)$ grows as $\left(\frac{3+\sqrt{5}}{2}\right)^n \approx 2.62^n$.

In the context of stirring with three stirrers we note that repeatedly performing the stirred motion g corresponding to $\sigma_1^{-1}\sigma_2$ is, in the sense of line stretching, the most efficient stirring protocol. More precisely, of all 'words' consisting of 2n letters, each letter a generator of the braid group B_3, the word $(\sigma_1^{-1}\sigma_2)^n$ yields an isotopy class for which the stretching factor is greatest. In more physical terms, if we are allowed to perform 2n switches, each of a pair of adjacent stirrers, we get the most stretching by using a 'pigtail' braid or, equivalently, an 'eggbeater' motion.

6.2 Experimental illustration

It is natural to illustrate the preceding theoretical developments by a simple experiment. Since previous work on chaotic advection has established that very viscous flows provide an almost ideal match between theory and experiment, we set up a system of three stirring rods in a cylindrical container of glycerol in which material lines can be marked by dye. A system of mechanical guides allows reproducible transposition of the two stirring rods on the right or on the left (producing the motions designated R and L in §3). At the outset the three rods are placed on a diameter. Each step of the stirring protocol consists in moving two rods such that they orbit one another on a circle centered halfway between them. At the end of such a step these two rods have interchanged positions. All motions are performed very slowly so that we may assume the fluid motion to be only due to the motion of the boundaries in the sense of a Stokes flow, i.e., no 'secondary fluid motions' were produced by the motion of the stirrers. When two rods have been interchanged and are again stationary, the fluid motion ceases immediately. The experimental setup is now ready for the next interchange of stirrers.

Dye was introduced into the apparatus, and photographs were taken through the flat bottom of the cylindrical container. Within the container the fluid motion is assumed to be largely two-dimen-

---

3) Note that $\mathbf{M}_g^n = \begin{pmatrix} F_{n+2} & F_{n+1} \\ F_{n+1} & F_n \end{pmatrix}$, with F_n the Fibonacci numbers 1, 1, 2, 3, 5, 8,... Thus, $\mathrm{Tr}(\mathbf{M}_g^n) = F_{n+2} + F_n$.

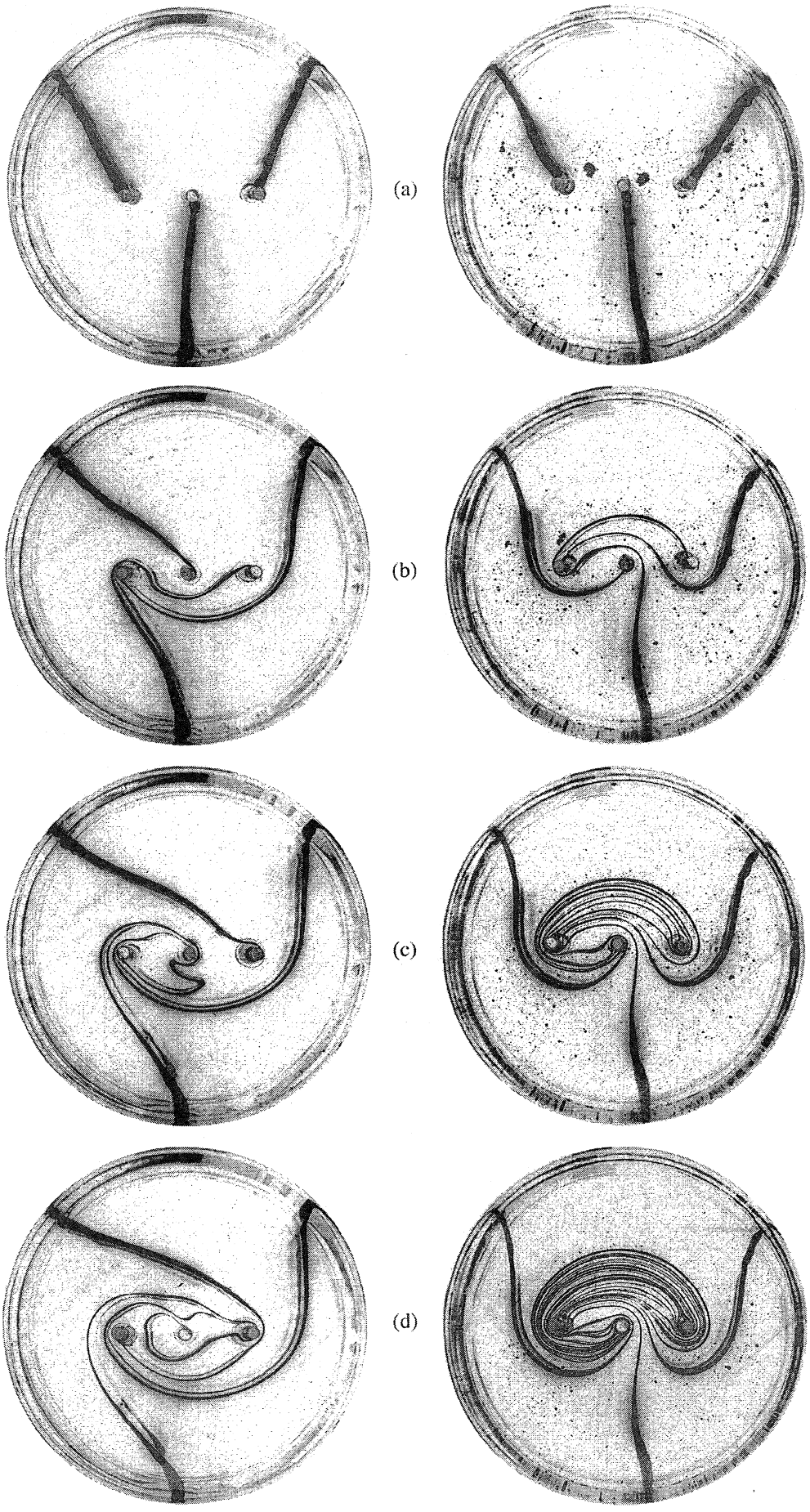

Figure 6.3: See caption next page.

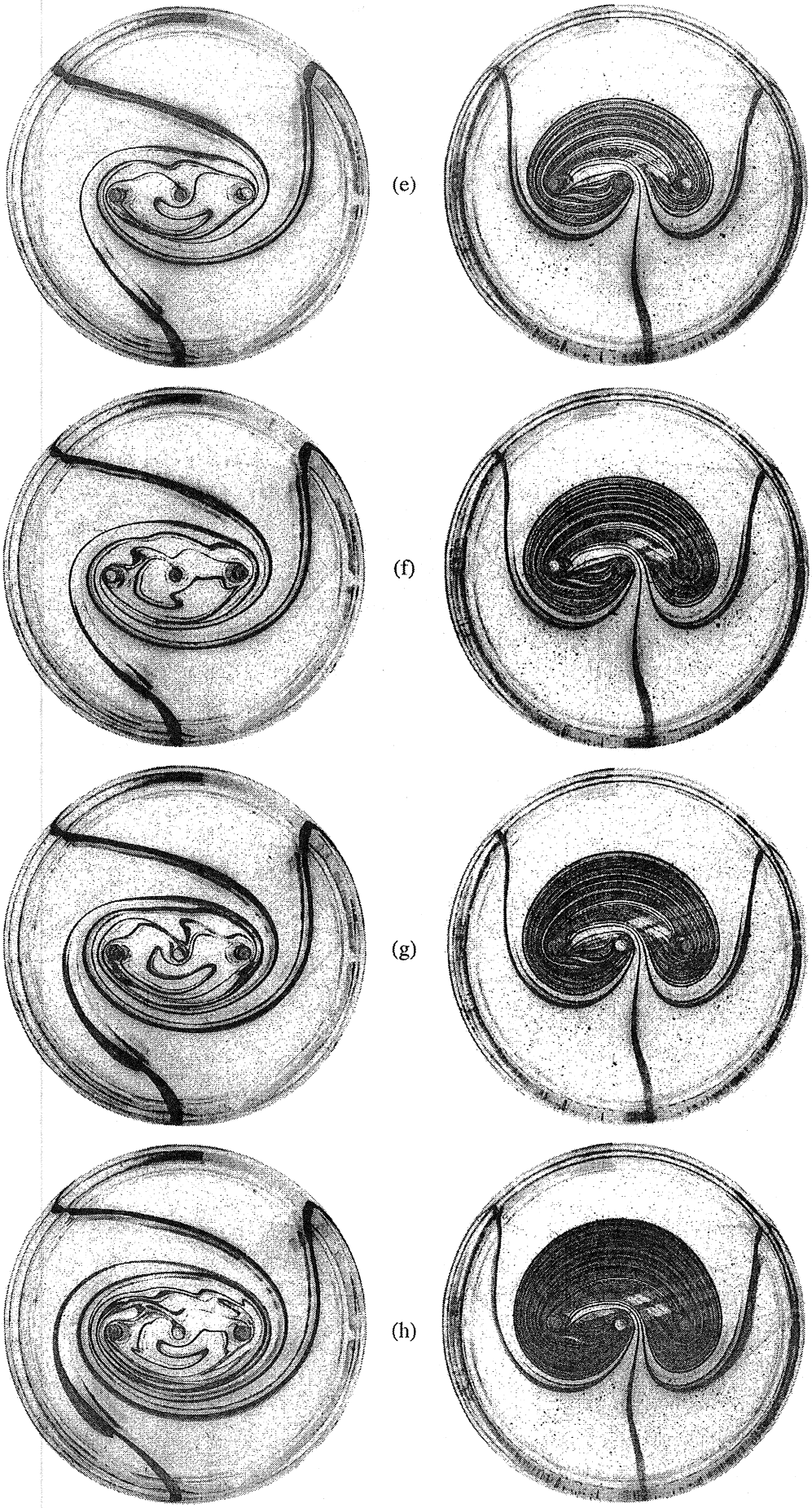

Figure 6.3: Experimental pictures of stirring by finite order (left) and pseudo-Anosov (right) protocols: (a) Initial condition. Configuration after (b) 1, (c) 2, (d) 3, (e) 4, (f) 5, (g) 6, and (h) 9 iterations.

sional, except near the top and bottom boundaries. In order to capture the motion in a planeperpendicular to the rods, we used a sheet of light to illuminate the dye and take pictures. The true fluid motion is, of course, not exactly two-dimensional, but the assumption of plane motion within most of the container seems adequate. The sheet of light would typically be positioned about halfway between the top and bottom surfaces of the fluid volume.

A sequence of snapshots of such dye line configurations for the two stirring protocols designated *f* and g in the preceding discussion are shown in Fig.6.3 [4]. Although the experiment is extremely simple in concept, and is not particularly difficult in practice, the results provide quite convincing evidence that dramatically different types of fluid stirring and mixing are taking place depending on the chosen stirring protocol. From a practical point of view these two ways of stirring the fluid are entirely equivalent in terms of energy requirements, and a mechanism that accomplishes one stirring protocol can easily be adapted to accomplish the other. The amount of stretching and close layering of material lines is clearly much greater in the pA case than in the finite order case, although the finite order case most certainly displays chaotic advection in the usual sense of the term (see also the discussion in §7). Furthermore, in the pA case a very interesting self-similar structure – shaped somewhat like an inverted heart – emerges. This structure corresponds to the invariant, unstable foliation of a pA map (see Appendix). It appears to have a cusp at the bottom where fluid is entering it. It would be interesting to develop a method for calculating this shape, even approximately. Remarkably, the structure is devoid of large elliptic islands. (TN theory, being strictly topological, does not predict this.) After just a few iterations the individual streaks of dye are so thin and so close together that a substantial amount of diffusion and blurring of individual lines must be taking place. In this sense the physical experiment in the pA case is not reversible after even three or four iterations, whereas the finite order case maintains clearly distinct material lines even up to nine iterations.

7. Discussion and conclusions

The present paper provides an application of a major result of modern topology to the problem of stirring of a fluid. We have shown in outline how Thurston-Nielsen theory applies to a prototypical problem of the type indicated in Fig.2.1. There are several additional mathematical details of TN theory that can be elaborated and that may be of physical significance. There are many other physical situations in which the topological tools presented here may be applicable. In this final section we mention a number of topics that fall under one or the other of these headings.

7.1 *Generalized horseshoe maps*

It has long been recognized that stretching and folding is central to the creation of chaos. The simplest example of this behavior is provided by what is known as *Smale's horseshoe map.* In the context of chaotic advection studies it has been suggested that horseshoes are the 'engines' of mixing. To discuss connections of horseshoes with TN theory we need to establish some terminology and review some mathematical background (for additional information see Franks 1982; Guckenheimer & Holmes 1983; Devaney 1989; Katok & Hasselblatt 1995).

By Smale's horseshoe (HS) map, H, we mean a specific diffeomorphism of the disk that is constructed by taking a rectangle, stretching it, folding it into a horseshoe shape, and then placing

4) There appear to be some 'double lines' in Fig. 6.3. These are due to optical reflections.

that folded structure over the original rectangle. The resulting diffeomorphism contains an invariant set, X, that is uniformly hyperbolic, i.e., H uniformly stretches in one direction and contracts in the other, and these stable and unstable directions line up under iteration. The set X contains all the periodic points (except a single attracting fixed point), and, indeed, all the so-called non-wandering points. The rectangles that are used for the construction can be used to code the dynamics as all possible sequences of 0 and 1. In other words, they form a Markov partition with transition matrix

$$\mathbf{N} = \begin{pmatrix} 1 & 1 \\ 1 & 1 \end{pmatrix}. \tag{7.1}$$

The eigenvalues 2 and $\frac{1}{2}$ of the matrix N give Lyapunov exponents $\pm\log 2$, while the number of periodic points fixed by H^n is given by[5] $\mathrm{Tr}(\mathbf{N}^n) = 2^n$.

A *generalized horseshoe map* (GHS) refers to a construction that is similar to Smale's HS, but one allows any number of rectangles that stretch and fold over themselves in a perhaps topologically complex manner (see Fig.A.2 in the Appendix for an example). As with Smale's HS, there is a compact, invariant set, X, on which the dynamics can be coded using the boxes as a Markov partition, but in this case we have as many symbols as boxes and some transitions may not be allowed. For simplicity we restrict the box-pulling so that X is indecomposable, i.e., has a dense orbit. This will happen if the transition matrix has an iterate that is strictly positive. Once again, the eigenvalues of the transition matrix give the Lyapunov exponents and the growth rate of the number of periodic points. Further, the structure of the invariant manifold template, i.e., the stable and unstable foliations, can be read off using the symbolic dynamics and the box-pulling picture.

In certain contexts the invariant set X is called the generalized horseshoe, and in others the map itself is given that name. In Smale's original terminology (Smale 1967) the set X is an example of a basic set, and the GHS is an *Axiom A diffeomorphism.* Whatever the terminology these maps or sets are the most common models for chaos – the dynamics are very complicated, yet may be understood using the symbolic description.

The GHS provides a somewhat different way to view TN theory: Start with a given diffeomorphism and begin performing continuous deformations of the map. For a stirred motion we may think of changing the parameters of the stirring protocol (but not its braid!) and applying an external, distributed force-field. The goal of all these deformations is to reduce or simplify the overall dynamics of the diffeomorphism. For example, we may squeeze down elliptic islands and move their eigenvalues so that they become flip saddles (i.e., saddles with negative eigenvalues); we may eliminate any sink-saddle pairs via saddle-node bifurcations; and we may reverse period-doubling (or, in general, period-multiplying) bifurcations. Since we are performing continuous deformations, all the resulting maps are in the same isotopy class, but what is left if and when the process terminates? And, if we perform the simplification process in different ways, do we get essentially different maps at the end? From the point of view of dynamics, the heart of TN theory is the answer to these questions. The simplest final map is the TN representative, and because it arises as the essentially unique termination of the simplification process, its dynamics must be

5) $\mathrm{Tr}(\mathbf{N}) = 2$, and since $\mathbf{N}^2 = 2\mathbf{N}$, it follows that $\mathbf{N}^n = 2^{n-1}\mathbf{N}$, and so $\mathrm{Tr}(\mathbf{N}^n) = 2^{n-1}\mathrm{Tr}(\mathbf{N}) = 2^n$.

present in every diffeomorphism in its isotopy class.

In simple domains, e.g., when there are zero, one or two stirrers in the disk, the dynamics can always be reduced to something simple and non-chaotic. But in other isotopy classes, the simplest map is chaotic, and so we attempt to make it hyperbolic so that its dynamics can be understood. The usual procedure in TN theory is to make the simplest map pA, in which case it is hyperbolic everywhere except for a finite number of singularities. However, we could just as well make the simplest map a GHS. The GHS has the advantage of providing a clearer visualization: the invariant manifold template is obvious, and the symbolic coding is unique (in pA maps a small set of points is multiply coded). It has the disadvantage of sometimes having a few extra periodic points. Let us call the simplest GHS in an isotopy class its *Axiom A representative.*[6] Figure A.2 shows the Axiom A representative in the isotopy class of our pA stirring protocol.

Now, in general, each isotopy class contains many GHS's. In fact, the Birkhoff-Smale theorem says that a GHS is always present when there is a transverse heteroclinic or homoclinic intersection. GHS's are thus a ubiquitous signature of chaos. What is special about the Axiom A representative is that the structure of its GHS is intrinsic to the isotopy class. The way its Markov boxes are pulled exactly characterizes the topology that distinguishes its isotopy class from any other. One way to view the persistence of the Axiom A representative's dynamics is that *every* map in its isotopy class has 'boxes' that are pulled in a topologically identical way. This is why the periodic orbits and, indeed, all the dynamics of the pA map, are present in every isotopic map. And, to repeat a point made earlier, this is why we use the term 'topological chaos' to describe maps isotopic to pA maps.

In contrast, Smale's HS is isotopic to the identity, and thus its dynamics can be removed via isotopy. Similar remarks hold for all the GHS's that one gets from heteroclinic and homoclinic intersections. These maps are undeniably chaotic, but the chaos has a relation to the ambient topology that is fundamentally different from that of the Axiom A representative.

This distinction is made especially clear by examining the behavior of simple loops under iteration. As discussed in §3, these converge to the unstable foliation of the pA map. Topologically this is identical to their converging to the unstable manifold template of the Axiom A representative. This is expected behavior when iterating the Axiom A representative, but the convergence holds for any isotopic diffeomorphism, and this illustrates another facet of the preservation of the invariant manifold template.

Finally, it is important to note that the theory does not say that every map in the isotopy class has the same GHS as the Axiom A representative (see Handel's theorem in §4.1). Rather, it could have something bigger (but not smaller), and there is no information obtained from the theory about the hyperbolicity of dynamics of the stirred motion.

7.2 *Connection to Melnikov's method*

The general class of techniques that goes under the name of Melnikov methods are perhaps the most common method for showing that a system is chaotic. Both the Melnikov method and TN theory yield the existence of GHS in the dynamics, but the details of their application and the conclusions obtained are quite different.

The simplest case of application of the Melnikov method is to a periodically forced, two-dimensional ODE, e.g., time-dependent advection in 2D flow. One usually studies the time-T

6) One can also choose a map in the class with a hyperbolic strange attractor, see Appendix.

diffeomorphism induced on the plane, where T is the period of the forcing. A parameter controls the magnitude of the forcing. When there is no forcing, the ODE is required to have a homoclinic (or heteroclinic) loop. After forcing, the Melnikov function measures (to first order) the crossing of stable and unstable manifolds, which were coincident at zero forcing. If this function crosses zero transversally, there is a transverse, homoclinic intersection for the time-T map. Thus, the Birkhoff-Smale theorem tells us that a GHS is embedded in the dynamics.

The method is very powerful because it allows one to do analytic calculations on explicit systems, the result of which can give very interesting information about the dynamics. There are many variants and refinements of the method (Wiggins 1990) and it has been extended to give additional information, such as lobe size, that is important in transport problems (Wiggins 1992; Beigie, Leonard & Wiggins 1995). One of the main shortcomings of the method is that it is perturbative. One must begin with a system (perhaps resulting from an averaging process) in which there is an analytically known homoclinic (or heteroclinic) loop, and the computations of the method only work rigorously for small perturbations. In addition, the GHS that one obtains will always be confined to a band around the unperturbed homoclinic or heteroclinic loop. The GHS are never topologically intrinsic; they can always be deformed away. In fact, the method explicitly shows how this can happen, namely, by reversing the deformation to regain the original homoclinic or heteroclinic connection. Thus, the Melnikov method never yields topological chaos in the sense of this paper.

In contrast, TN theory gives dynamics that are topologically intrinsic, and holds for deformations of any size (within the isotopy class). The GHS from the Melnikov method are hyperbolic, whereas the TN representative is only known to be semiconjugate to a GHS. On the other hand, TN theory gives a great deal more information about the dynamics of the GHS, since it yields the Axiom A representative. Thus, one gets such information as the number of periodic points, stretching rates, invariant manifold templates, and so on.

An obvious shortcoming of TN theory is that it only yields information if the map in question is in a pA isotopy class, which is often not the case. In fact, the domain in which the diffeomorphism is defined must be sufficiently complicated for a pA class to even exist. (There is, however, a well developed theory in which one removes known periodic orbits from the domain, thereby creating the necessary topological complexity; see Boyland 1994, and Hall 1993). On the other hand, computing the type of an isotopy class is very robust, and needs only a small amount of combinatorial data about the map, e.g., its braid.

A crucial restriction of TN theory is that it only works for diffeomorphisms in two dimensions, whereas Melnikov's method works in any dimension (although the theory and the computations become more difficult in higher dimensions). Both TN theory and Melnikov's method only give a lower bound on the dynamical complexity of the system being analyzed. They give no control, for example, over the total area occupied by elliptic islands in an area-preserving diffeomorphism. Such information is typically very important to the mixing efficiency of a map.

7.3 *Other applications*

We have considered the application of TN theory to a relatively simple case of 'batch mixing' of a viscous fluid and we have studied two protocols with three stirrers in detail. TN theory applies to more stirrers as well, and there is much to be explored with reference to such 'metric issues' as optimizing the mixed region by using specially shaped containers, varying the stirrer

diameter and its trajectory, and so on.

The stirring problem discussed here was not the first to which we applied the theory. Much as the original introduction of the concept of chaotic advection (Aref 1984) was motivated by consideration of advection by three point vortices on the infinite plane (the 'restricted' four-vortex problem) by Aref & Pomphrey (1980, 1982), we were first led to apply TN theory to the problem of advection by three point vortices of total strength zero. The vortices play the role of stirrers – with the hydrodynamics being that of ideal flow rather than Stokes flow – and one can consider braids and isotopy classes of the advecting motion produced by the three dynamically interacting point vortices. On the infinite plane the vortex dynamics problem was solved in detail some years ago (Rott 1989; Aref 1989). There are four distinct regimes of motion. We have checked that in all cases the map for the advection of a passive particle by the three vortices is in a finite order isotopy class, or a reducible class with all finite order components.

Recently, we have generalized the method of solution to three point vortices in a periodic strip (Aref & Stremler 1996) and to three vortices in a periodic parallelogram (Stremler & Aref 1996). In the former case one has to impose the condition that the vortices have total strength zero; in the latter this follows from the periodicity of the flow. With either type of periodic boundary condition we find some regimes of motion that lead to advection isotopic to a pA map, and for such regimes we can apply the apparatus of TN theory. We hope to report separately on this application.

It is also possible to use the results obtained here to design efficient 'static' mixers for steady flow in tubes. If we imagine inserting a set of three strands inside a straight tube, the mapping of inlet to outlet will play the role of our 2D diffeomorphism, and the braid formed by the strands can be chosen to make this diffeomorphism isotopic to a pA map, which will imply more efficient transverse mixing. Since it is the topology and not the size of the tubes that matters, it may be possible to enhance mixing by keeping the inserted strands relatively thin, thus avoiding the large pressure drops that often arise in mixers of this type.

The mechanism of producing topological chaos introduced here involves motions on the scale of the overall motion of the system of stirrers. Thus, one may hope that the chaotically stirred region will be of a scale set by the configuration of the stirrers and their motions, i.e., a scale that is largely under the control of the designer of the apparatus. This is certainly the case in the simple experimental illustration given above, where the chaotic region fills a region within the container of about the size one would expect based on the paths of the stirrers. In prior illustrations of chaotic advection the scale of the chaos always arises through the dynamic response of the fluid to the in-place motion of inner and outer boundaries, and the scale on which advective chaos is seen depends on the 'tuning' of some control parameter, and is difficult to anticipate or predict.

Acknowledgements

We thank V. V. Meleshko for discussions and S. T. Thoroddsen for access to laboratory facilities and for help in constructing the experimental apparatus. This work was supported in part by NSF grant CTS-9311545. MAS acknowledges the support of an ONR graduate fellowship.

References

Aref, H. 1984 Stirring by chaotic advection. *J. Fluid Mech.* **143**, 1-21.

Aref, H. 1989 Three-vortex motion with zero total circulation: Addendum. *J. Appl. Math. Phys. (ZAMP)* **40**, 495-500.

Aref, H. 1990 Chaotic advection of fluid particles. *Phil. Trans. Roy. Soc. (London) A* **333**, 273-289.

Aref, H. 1991 Stochastic particle motion in laminar flows. *Phys. Fluids A* **3**, 1009-1016.

Aref, H. (ed.) 1994 *Chaos Applied to Fluid Mixing.* Special issue of *Chaos, Solitons & Fractals* **4**, 380pp.

Aref, H. & Pomphrey, N. 1980 Integrable and chaotic motions of four vortices. *Phys. Lett. A* **78**, 297-300.

Aref, H. & Pomphrey, N. 1982 Integrable and chaotic motions of four vortices I: The case of identical vortices. *Proc. Roy. Soc. (London) A* **380**, 359-387.

Aref, H. & Balachandar, S. 1986 Chaotic advection in a Stokes flow. *Phys. Fluids* **29**, 3515-3521.

Aref, H., Boyland, P. L. & Stremler, M. A. 1996 Topological fluid mechanics of stirring: Applications. *Bull. Amer. Phys. Soc.* **41**, 1683.

Aref, H. & Stremler, M. A. 1996 On the motion of three point vortices in a periodic strip. *J. Fluid Mech.* **314**, 1-25.

Arnol'd, V. I. and Avez, A. 1968 *Ergodic Problems of Classical Mechanics.* Benjamin.

Beigie, D., Leonard, A., & Wiggins, S. 1995 Invariant manifold templates for chaotic advection. *Chaos, Solitons & Fractals* **4**, 5--124.

Bestvina, M. & Handel, M. 1995 Train-tracks for surface homeomorphisms. *Topology* **34**, 109--140.

Birman, J. 1975 *Braids, Links and Mapping Class Groups.* Annals of Mathematics Studies, Princeton University Press.

Birman, J. & Williams, R. 1983 Knotted periodic orbits in dynamical systems II: Knot holders for fibered knots. *Contemp. Math.*, 20 1--60.

Boyland, P. 1994 Topological methods in surface dynamics. *Topology and Appl.* **58**, 223-298.

Boyland, P. L., Aref, H. & Stremler, M. A. 1996 Topological fluid mechanics of stirring: Theory. *Bull. Amer. Phys. Soc.* **41**, 1683.

Boyland, P. & Franks, J. 1989 *Notes on dynamics of surface homeomorphisms: Lectures by P. Boyland and J. Franks, notes by C. Carroll, J. Guaschi and T. Hall.* University of Warwick preprint, 1-48.

Casson, A. & Bleiler, S. 1988 Automorphisms of surfaces after Nielsen and Thurston. *London Math. Soc. Stud. Texts* **9**. Cambridge University Press.

Chaiken, J., Chevray, R., Tabor, M. & Tan, Q. M. 1986 Experimental study of Lagrangian turbulence in a Stokes flow. *Proc. Roy. Soc. (London) A* **408**, 165-174.

Coxeter, H. & Moser, W. 1972 *Generators and Relations for Discrete Groups.* Third edition. Springer-Verlag.

Devaney, R. 1989 *An Introduction to Chaotic Dynamical Systems.* Addison-Wesley.

Fathi, A., Lauderbach, F. & Poenaru, V. 1979 Travaux de Thurston sur les surfaces. *Asterique,* 66-67.

Franks, J. 1970 *Anosov diffeomorphisms.* AMS Proceedings of Symposia in Pure Mathematics **XIV**, 61--93 .

Franks, J. 1982 *Homology and Dynamical Systems.* CBMS Lectures **49**, American Mathematical Society.

Franks, J. & Misiurewicz, M. 1993 Cycles for disk homeomorphisms and thick trees. *Contemp. Math.* **152**, 69--139.

Guckenheimer, J. & Holmes, P. 1983 *Nonlinear Oscillations, Dynamical Systems, and Bifurcations of Vector Fields.* Springer-Verlag.

Hall, T. 1993 Weak universality in two-dimensional transitions to chaos. *Phys. Rev. Lett.* **71** , 58--61.

Handel, M. 1985 Global shadowing of pseudo-Anosov homeomorphisms. *Ergod. Th. & Dyn. Sys.* **5**, 373--377.

Jana, S. C., Metcalfe, G. & Ottino, J. M. 1994 Experimental and computational studies of mixing in complex Stokes flows: the vortex mixing flow and multicellular cavity flows. *J. Fluid Mech.* **269**, 199-246.

Katok, A. 1979 Bernoulli diffeomorphisms on surfaces. *Ann. Math.* **110**, 529--547.

Katok, A. & Hasselblatt, B. 1995 *Introduction to the modern theory of dynamical systems.* Encyclopedia of Mathematics and its Applications **54**.

Los, J. 1993 Pseudo-Anosov maps and invariant train tracks in the disc: a finite algorithm. *Proc. London Math. Soc.* **66**, 400--430.

Lundsgaard-Hansen, V. 1993 Jakob Nielsen (1890-1959). *Math. Intelligencer* **15**(4), 44-53.

MacKay, R. S. 1990 Postscript: Knots for three-dimensional vector fields. In *Topological Fluid Mechanics,* H. K. Moffatt and A. Tsinober (eds.), Cambridge University Press, p.787.

McRobie, F. A. and Thompson, J. M. T. 1993 Braids and knots in driven oscillators. *Intern. J. Bifurcation & Chaos* **3**, 1343-1361.

Moffatt, H. K. and Tsinober, A. (eds.) 1990 *Topological Fluid Mechanics.* Cambridge University Press.

Ottino, J. M. 1989 *The kinematics of mixing: Stretching, chaos and transport.* Cambridge University Press.

Ottino, J. M. 1990 Mixing, chaotic advection and turbulence. *Ann. Rev. Fluid Mech.* **22**, 207-253.

Ricca, R. L. & Berger, M. A. 1996 Topological ideas and fluid mechanics. *Physics Today* **49**(12), 28-34.

Robinson, C. 1995 *Dynamical systems: stability, symbolic dynamics, and chaos.* Studies in Advanced Mathematics. CRC Press.

Rott, N. 1989 Three-vortex motion with zero total circulation. *J. Appl. Math. Phys. (ZAMP)* **40**, 473-494.

Seifert, H. & Threlfall, W. 1980 *A Textbook of Topology.* Academic Press.

Smale, S. 1967 *Differentiable dynamical systems. Bull. Amer. Math. Soc.* **73**, 747--817.

Stremler, M. A. & Aref, H. 1996 Motion of three point vortices in a periodic domain. *Bull. Amer. Phys. Soc.* **41**, 1757.

Thurston, W. 1988 On the geometry and dynamics of diffeomorphisms of surfaces. *Bull. Amer. Math. Soc.* **19**, 417-431.

Wiggins, S. 1990 *Introduction to applied nonlinear dynamical systems and chaos.* Texts in Applied Mathematics **2**. Springer-Verlag.

Wiggins, S. 1992 *Chaotic transport in dynamical systems.* Interdisciplinary Applied Mathematics **2**. Springer-Verlag.

Appendix: Isotopy classes on the torus and on $\mathbf{R}_3$.

In the case of three stirrers or, equivalently, isotopy classes of diffeomorphisms of R_3, virtually all aspects of the Thurston-Nielsen theory can be computed explicitly and fairly easily. This is because of the close connection between these isotopy classes and linear automorphisms of the two-torus. This connection is fairly well known mathematical 'folklore'. It was used to study isotopy classes in Birman (1975) and for dynamics by Katok (1979), Birman & Williams (1983), Boyland & Franks (1989), and others. The pA map corresponding to the cat map (and represented by the braid $\sigma_1^{-1}\sigma_2$) is a well known example. Indeed, W. Thurston and D. Sullivan painted a picture of its 'advection' pattern across from the elevators on the 7th floor of the Berkeley Mathematics Department in 1971!

As described in §4, we obtain a map ϕ_M on the torus by projecting the linear map on the plane derived from an integer matrix

$$\mathbf{M} = \begin{pmatrix} a & b \\ c & d \end{pmatrix}. \tag{A.1}$$

In our discussion here we still require ad – bc = 1, but we put no restrictions on the sign of the integers or on the value of the trace.

The first result is that an isotopy class of diffeomorphisms on the two-torus contains exactly one linear automorphism ϕ_M (isotopy of diffeomorphisms on the torus is defined analogously to that on the regions R_k). In Thurston-Nielsen theory, this linear automorphism is the TN representative in its class. Further, the trace of the matrix **M** determines the type of the TN representative. If |Tr(M)| >2, we are in the Anosov case discussed in §4.2 (an Anosov map is also considered to be pA). If |Tr(M)| < 2, one checks that for n = 3, 4 or 6, $\mathbf{M}^n = \mathbf{1}$, the unit matrix, and so $(\phi_M)^n$ is the identity map[7]. These are all finite order cases. Finally, if Tr(M) = ± 2, **M** is

7) The point is that ad – bc = 1 implies $\mathbf{M}^2 = \mathrm{Tr}(\mathbf{M})\,\mathbf{M} - \mathbf{1}$. Thus, Tr(M) = 0 implies $\mathbf{M}^2 = -\mathbf{1}$, and $\mathbf{M}^4 = \mathbf{1}$. For Tr(M) = 1, $\mathbf{M}^2 = \mathbf{M} - \mathbf{1}$, $\mathbf{M}^3 = \mathbf{M}^2 - \mathbf{M} = -\mathbf{1}$, and $\mathbf{M}^6 = \mathbf{1}$. Finally, for Tr(M) = –1, $\mathbf{M}^2 = -\mathbf{M} - \mathbf{1}$, $\mathbf{M}^3 = \mathbf{1}$.

either 1, –1 (two more finite order cases), or is similar to a matrix of the form $\begin{pmatrix} 1 & b \\ 0 & 1 \end{pmatrix}$. This is the reducible case, since ϕ_M leaves invariant the loop in the torus corresponding to the vector (1,0).

The next step is to connect these torus maps to homeomorphisms on R_3. We begin by recalling the construction of the toral map ϕ_M (see §4.2). Let f_M be the map of the plane induced by the matrix M. Now,

$$f_M(x + n, y + m) = f_M(x, y) + (n', m') \tag{A.2}$$

for some integers n' and m'. Thus, by reducing modulo 1 in both coordinates, f_M induces a map ϕ_M on the unit square with opposite sides identified. This identification yields a topological torus, which concludes the topological description of the construction. To express it in formulae, start by letting e(x,y) = (exp(2πix), exp(2πiy)) and consider e to be a map from the plane to the torus. The inverse of e, denoted e^{-1}, is multi-valued but the definition $\phi_M = e\, f_M\, e^{-1}$ makes sense because of (A.2), which says that the choice of the value of e^{-1} does not matter.

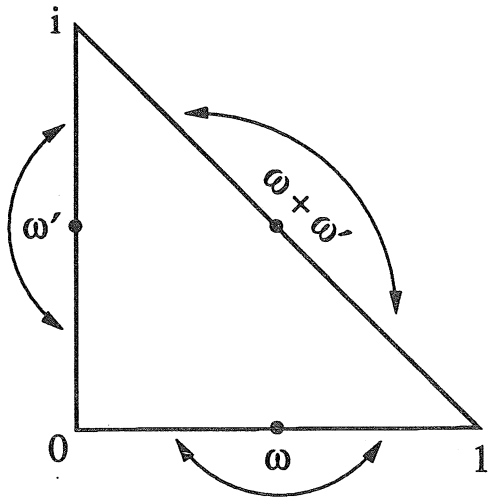

Figure A.1: Obtaining the sphere via identification of a pair of subarcs in each side of a triangle.

Next we see how similar considerations allow us to use f_M to induce a map of the sphere S^2. Equation (A.2) can be viewed as expressing a symmetry of the map f_M. Note that f_M has another symmetry, namely,

$$f_M(-x, -y) = f_M(x, y). \tag{A.3}$$

This means that we can project f_M to a map Φ_M defined on the space where we reduce points in the plane modulo integers *and* we treat a point and its opposite as the same. Equivalently, f_M induces a map on the space that we get by identifying opposing edges of the unit square as well as pairs of points that correspond under S, where S is the rotation of the unit square by π about its center. This space is obtained from the triangle with vertices (0, 0), (1, 0) and (0,1) with the side identifications as indicated in Figure A.1. This identification yields the sphere, so we have given

the topological description of the construction of the homeomorphisms of the sphere. To express this construction in formulae, the role of the projection e used in the torus case may be played by a Weierstrass $\wp$ function. Recall that $\wp$ is doubly periodic – we fix the periods to be $2\omega = 1$ and $2\omega' = i$, so that $\wp$'s (double) poles are all on the integer lattice. We use the notation $\wp$ for the function obtained with these particular choices. Note that $\wp$ may be viewed as a map from the plane to the Riemann sphere S^2, or alternatively, from the torus to S^2. Now we define a homeomorphism of the sphere by $\Phi_M = \wp f_M \wp^{-1}$. Once again, $\wp^{-1}$ is multi-valued, but the double periodicity of $\wp$ and the symmetry, $\wp(-z) = \wp(z)$, coupled with (A.2) and (A.3), show that the choice of the value of $\wp^{-1}$ does not matter.

We have now obtained from f_M a diffeomorphism on the sphere S^2 and we want to use it to obtain a diffeomorphism on the region R_3. For this, the first necessary observation is that the point (0,0) remains fixed under any map f_M, and so the corresponding point on the sphere, $\wp(0) = \infty$, is a fixed point of Φ_M. Thus we may remove ∞ from S^2 and the map Φ_M still makes sense because $\Phi_M(\infty) = \infty$. A disk may be obtained by replacing the point removed with a circle. We can still think of Φ_M as defined on this disk if we take care with the definition on the boundary circle.

One final observation is necessary to obtain a diffeomorphism of R_3. The three points $e_1 = \wp(\omega) = \wp(\frac{1}{2})$, $e_2 = \wp(\omega + \omega') = \wp(\frac{1+i}{2})$, and $e_3 = \wp(\omega') = \wp(\frac{i}{2})$ are permuted by Φ_M, since for any matrix $\mathbf{M}$ of the type considered here

$$\mathbf{M}\begin{pmatrix} \frac{m}{2} \\ \frac{n}{2} \end{pmatrix} = \begin{pmatrix} \frac{am+bn}{2} \\ \frac{cm+dn}{2} \end{pmatrix}, \tag{A.4}$$

and the condition $ad-bc = 1$ implies that the numerators cannot both be even unless m and n are both even. So, we may also remove the three additional points e_1, e_2, and e_3 and replace them with circles that are permuted by Φ_M. Thus we obtain a homeomorphism on R_3 that we shall denote Ψ_M.

Recalling that we may also think of $\wp$ as a map from the torus to S^2, we see that we could also define $\Phi_M = \wp \phi_M \wp^{-1}$. Thus, Ψ_M can be completely understood from the corresponding toral automorphism ϕ_M. In particular, each Ψ_M will be the TN representative in its isotopy class and its TN type will be the same as the corresponding toral automorphism ϕ_M. Furthermore, each isotopy class contains a diffeomorphism Ψ_M, but note that as a consequence of (A.3) $\mathbf{M}$ and $-\mathbf{M}$ will yield the same map on the sphere.

The main result of these considerations is that to determine the TN type of an isotopy class on R_3, we just need to determine the Ψ_M in that class. The key to finding the appropriate $\mathbf{M}$ lies in the connection between the braid group coordinates for isotopy classes and the algebraic structure of the collection of matrices $\mathbf{M}$. The algebraic fact that we need is that any matrix $\mathbf{M}$ of the type we have been considering here can be written as a product

$$\mathbf{M} = \mathbf{L}^{n_1} \mathbf{R}^{n_2} \ldots \mathbf{L}^{n_{k-1}} \mathbf{R}^{n_k}, \tag{A.5a}$$

where $\mathbf{R}$ and $\mathbf{L}$ are the matrices M_2 and M_1, respectively, from §6,

$$\mathbf{R} = \begin{pmatrix} 1 & 0 \\ 1 & 1 \end{pmatrix} \quad ; \quad \mathbf{L} = \begin{pmatrix} 1 & -1 \\ 0 & 1 \end{pmatrix}; \tag{A.5b}$$

and the n_i are positive or negative integers, and we allow $n_1 = 0$ or $n_k = 0$ (Coxeter & Moser, 1972, p.85). The induced maps, Ψ_R and Ψ_L, respectively, provide the key to connecting the matrix $\mathbf{M}$ to the isotopy class of Ψ_M and its braid description.

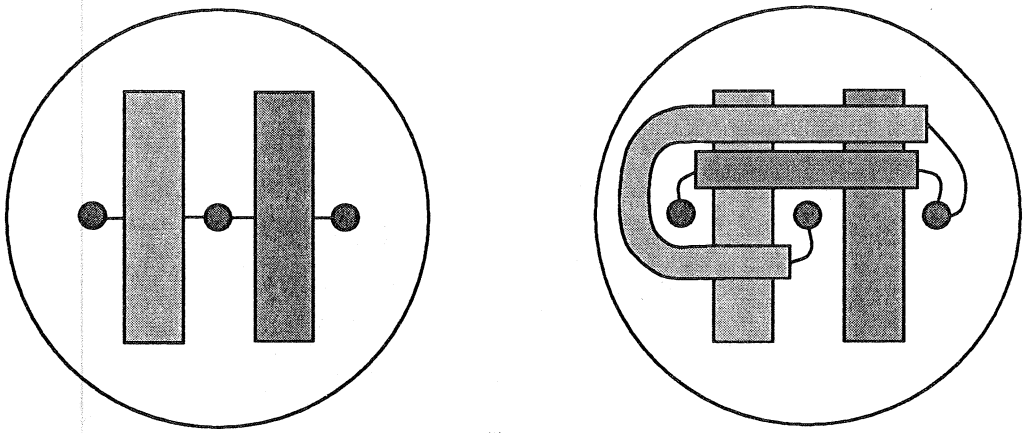

Figure A.2: The motion of the Markov boxes in the Axiom A representative in the class of the pseudo-Anosov stirring protocol.

In order to understand the braids of the maps Ψ_R and Ψ_L we need to see how they move the points e_1, e_2 and e_3. These points are the constants designated by the same symbols in the theory of elliptic functions. With our choice of periods it turns out that $e_2 = 0$, and e_1 and e_3 are both real with $0 < e_1 = -e_3$ (≈ -1.72). Now, viewing the plane from the negative real axis, one checks that Ψ_L yields an isotopy class with braid description σ_1, while Ψ_R yields σ_2. The correspondence of matrices to braids respects multiplication, i.e., the matrix corresponding to $\mathbf{M}$ in (A.5a) is the braid

$$\beta_M = \sigma_1^{n_1} \sigma_2^{n_2} \ldots \sigma_1^{n_{k-1}} \sigma_2^{n_k}. \tag{A.5c}$$

We would like to invert this process, namely for a braid β written in terms of the generators we replace each occurrence of σ_1 by $\mathbf{L}$ and each occurrence of σ_2 by $\mathbf{R}$ (and similarly for inverses) and so obtain a matrix $\mathbf{M}$ such that Ψ_M has isotopy class 'coordinates' β_M. For this to make sense we need to check that braids that are equal (for example $\sigma_1\sigma_2\sigma_1 = \sigma_2\sigma_1\sigma_2$) yield the same matrix. This is a straightforward computation. Recall also that our braid coordinates were only defined up to full twists around the outer boundary, i.e., up to multiplication by a power of $(\sigma_1\sigma_2)^3$. The matrix corresponding to $(\sigma_1\sigma_2)^3$ is minus the identity matrix, so its presence will not influence the absolute value of the trace of $\mathbf{M}$. Thus, for example, the braid $\sigma_1^{-1}\sigma_2$ corresponds to the matrix $\mathbf{L}^{-1}\mathbf{R} = \begin{pmatrix} 2 & 1 \\ 1 & 1 \end{pmatrix}$, and $\sigma_1\sigma_2$ corresponds to $\mathbf{LR} = \begin{pmatrix} 0 & -1 \\ 1 & 1 \end{pmatrix}$ (cf. §6.1).

In summary then, given a stirring protocol with three stirrers, we generate a braid as described

in §6. After writing this braid in terms of the generators σ_1 and σ_2 we obtain the matrix M. The map Ψ_M is then isotopic to the stirring diffeomorphism generated by the protocol. Further, the trace of M determines the TN type of Ψ_M and thus of the isotopy class.

In particular, if $|\mathrm{Tr}(M)| > 2$, we are in the pseudo-Anosov case and we know that our stirred motion must have complicated topology and dynamics. The eigenvalues of M give the stretching factor. To understand the topology of the invariant manifold template it is usually easiest to study the Axiom A representative (as described in §7.1). We may construct this map using the arcs shown in Fig. 6.1(a). These arcs are 'fattened' into Markov boxes and then pulled as required by the topology. Figure A.2 shows the Axiom A representative in the class of our pA stirring protocol, i.e., for the braid $\sigma_1^{-1}\sigma_2$. The map in this isotopy class with a strange attractor is the Plykin map (cf. Guckenheimer & Holmes, 1983, p.264).

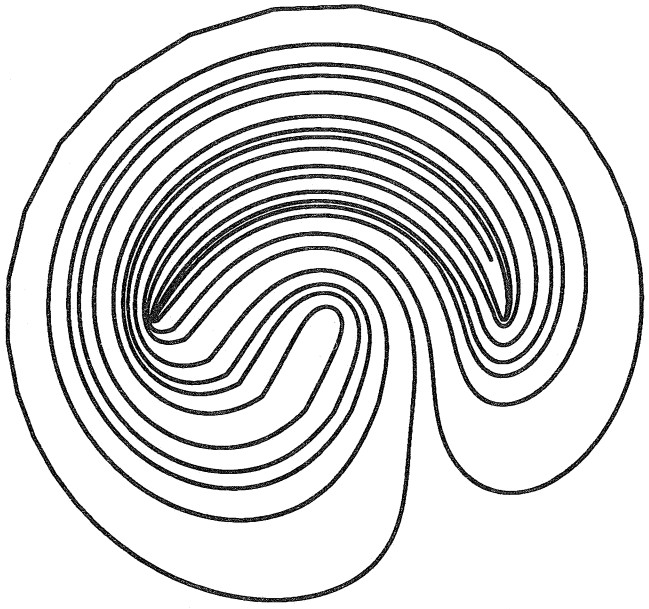

Figure A.3: An unstable manifold of the pseudo-Anosov map in the class of the pseudo-Anosov stirring protocol (compare Figure 6.3, right column).

Figure A.3 shows a portion of the unstable manifold of a point for the pA map represented by $\sigma_1^{-1}\sigma_2$. The picture was produced using the Weierstrass $\sqrt{}$ function to project an unstable manifold of the cat map (i.e., the unstable eigendirection) onto the plane. Since $\sqrt{}$ has poles, some rescaling was necessary. As noted in §4.2, under iteration by a pA map arcs, loops and sets converge to the unstable foliation. This property is shared by any map isotopic to the pA map. Thus, this structure should emerge under repetition of the pA stirring protocol in a physical fluid. A comparison of Fig. A.3 and the right column of Fig.6.3 clearly shows this to be the case.

List of Recent TAM Reports

No.	*Authors*	*Title*	*Date*
767	Piomelli, U.	Large-eddy simulation of turbulent flows	Sept. 1994
768	Harris, J. G., D. A. Rebinsky, and G. R. Wickham	An integrated model of scattering from an imperfect interface—*Journal of the Acoustical Society of America* **99**, 1315–1325 (1996)	Sept. 1994
769	Hsia, K. J., and Z.-Q. Xu	The mathematical framework and an approximate solution of surface crack propagation under hydraulic pressure loading—*International Journal of Fracture*, in press (1996)	Sept. 1994
770	Balachandar, S.	Two-point correlation and its eigen-decomposition for optimal characterization of mantle convection	Oct. 1994
771	Lufrano, J. M., and P. Sofronis	Numerical analysis of the interaction of solute hydrogen atoms with the stress field of a crack—*International Journal of Solids and Structures*, **33**, 1709–1723 (1996)	Oct. 1994
772	Aref, H., and S. W. Jones	Motion of a solid body through ideal fluid—Proceedings of the DCAMM 25th Anniversary Volume, 55–68 (1994)	Oct. 1994
773	Stewart, D. S., T. D. Aslam, J. Yao, and J. B. Bdzil	Level-set techniques applied to unsteady detonation propagation—In "Modeling in Combustion Science," *Lecture Notes in Physics* , eds. J. Buckmaster and J. Takeno **126**, 390–409 (1996)	Oct. 1994
774	Mittal, R., and S. Balachandar	Effect of three-dimensionality on the lift and drag of circular and elliptic cylinders—*Physics of Fluids* **7**, 1841–1865 (1995)	Oct. 1994
775	Stewart, D. S., T. D. Aslam, and J. Yao	On the evolution of cellular detonation	Nov. 1994 *Revised* Jan. 1996
776	Aref, H.	On the equilibrium and stability of a row of point vortices—*Journal of Fluid Mechanics* **290**, 167–181 (1995)	Nov. 1994
777	Cherukuri, H. P., T. G. Shawki, and M. El-Raheb	An accurate finite-difference scheme for elastic wave propagation in a circular disk—*Journal of the Acoustical Society of America*, in press (1996)	Nov. 1994
778	Li, L., and N. R. Sottos	Improving hydrostatic performance of 1–3 piezocomposites—*Journal of Applied Physics* **77**, 4595–4603 (1995)	Dec. 1994
779	Phillips, J. W., D. L. de Camara, M. D. Lockwood, and W. C. C. Grebner	Strength of silicone breast implants—*Plastic and Reconstructive Surgery* **97**, 1215–1225 (1996)	Jan. 1995
780	Xin, Y.-B., K. J. Hsia, and D. A. Lange	Quantitative characterization of the fracture surface of silicon single crystals by confocal microscopy—*Journal of the American Ceramics Society* **78**, 3201–3208 (1995)	Jan. 1995
781	Yao, J., and D. S. Stewart	On the dynamics of multi-dimensional detonation—*Journal of Fluid Mechanics* **309**, 225–275 (1996)	Jan. 1995
782	Riahi, D. N., and T. L. Sayre	Effect of rotation on the structure of a convecting mushy layer—*Acta Mechanica* **118**, 109–120 (1996)	Feb. 1995
783	Batchelor, G. K., and TAM faculty and students	A conversation with Professor George K. Batchelor	Feb. 1995
784	Sayre, T. L., and D. N. Riahi	Effect of rotation on flow instabilities during solidification of a binary alloy—*International Journal of Engineering Science* **34**, 1631–1645 (1996)	Feb. 1995
785	Xin, Y.-B., and K. J. Hsia	A technique to generate straight surface cracks for studying the dislocation nucleation condition in brittle materials—*Acta Metallurgica et Materialia* **44**, 845–853 (1996)	Mar. 1995
786	Riahi, D. N.	Finite bandwidth, long wavelength convection with boundary imperfections: Near-resonant wavelength excitation—*International Journal of Mathematics and Mathematical Sciences*, in press (1996)	Mar. 1995
787	Turner, J. A., and R. L. Weaver	Average response of an infinite plate on a random foundation—*Journal of the Acoustical Society of America* **99**, 2167–2175 (1996)	Mar. 1995

List of Recent TAM Reports (cont'd)

No.	Authors	Title	Date
788	Weaver, R. L., and D. Sornette	The range of spectral correlations in pseudointegrable systems: GOE statistics in a rectangular membrane with a point scatterer—*Physical Review E* **52**, 341 (1995)	Apr. 1995
789	Students in TAM 293–294	Thirty-second student symposium on engineering mechanics, J. W. Phillips, coordinator: Selected senior projects by K. F. Anderson, M. B. Bishop, B. C. Case, S. R. McFarlin, J. M. Nowakowski, D. W. Peterson, C. V. Robertson, and C. E. Tsoukatos	Apr. 1995
790	Figa, J., and C. J. Lawrence	Linear stability analysis of a gravity-driven Newtonian coating flow on a planar incline	May 1995
791	Figa, J., and C. J. Lawrence	Linear stability analysis of a gravity-driven viscosity-stratified Newtonian coating flow on a planar incline	May 1995
792	Cherukuri, H. P., and T. G. Shawki	On shear band nucleation and the finite propagation speed of thermal disturbances—*International Journal of Solids and Structures*, in press (1996)	May 1995
793	Harris, J. G.	Modeling scanned acoustic imaging of defects at solid interfaces—Chapter in *IMA Workshop on Inverse Problems in Wave Propagation*, eds. G. Chevant, G. Papanicolaou, P. Sacks and W. E. Symes, 237–258, Springer-Verlag, New York (1996)	May 1995
794	Sottos, N. R., J. M. Ockers, and M. J. Swindeman	Thermoelastic properties of plain weave composites for multilayer circuit board applications	May 1995
795	Aref, H., and M. A. Stremler	On the motion of three point vortices in a periodic strip—*Journal of Fluid Mechanics* **314**, 1–25 (1996)	June 1995
796	Barenblatt, G. I., and N. Goldenfeld	Does fully-developed turbulence exist? Reynolds number independence versus asymptotic covariance—*Physics of Fluids* **7**, 3078–3082 (1995)	June 1995
797	Aslam, T. D., J. B. Bdzil, and D. S. Stewart	Level set methods applied to modeling detonation shock dynamics—*Journal of Computational Physics*, **126**, 390–409 (1996)	June 1995
798	Nimmagadda, P. B. R., and P. Sofronis	The effect of interface slip and diffusion on the creep strength of fiber and particulate composite materials—Proceedings of the ASME Applied Mechanics Division **213**, 125–143 (1995)	July 1995
799	Hsia, K. J., T.-L. Zhang, and D. F. Socie	Effect of crack surface morphology on the fracture behavior under mixed mode loading—*ASTM Special Technical Publication* 1296, in press (1996)	July 1995
800	Adrian, R. J.	Stochastic estimation of the structure of turbulent fields—*Eddy Structure Identification*, ed. J. P. Bonnet, Springer: Berlin 145–196 (1996)	Aug. 1995
801	Riahi, D. N.	Perturbation analysis and modeling for stratified turbulence	Aug. 1995
802	Thoroddsen, S. T.	Conditional sampling of dissipation in high Reynolds number turbulence—*Physics of Fluids* **8**, 1333–1335	Aug. 1995
803	Riahi, D. N.	On the structure of an unsteady convecting mushy layer—*Acta Mechanica*, in press (1996)	Aug. 1995
804	Meleshko, V. V.	Equilibrium of an elastic rectangle: The Mathieu–Inglis–Pickett solution revisited—*Journal of Elasticity* **40**, 207–238 (1995)	Aug. 1995
805	Jonnalagadda, K., G. E. Kline, and N. R. Sottos	Local displacements and load transfer in shape memory alloy composites	Aug. 1995
806	Nimmagadda, P. B. R., and P. Sofronis	On the calculation of the matrix–reinforcement interface diffusion coefficient in composite materials at high temperatures—*Acta Metallurgica et Materialia*, **44**, 2711–2716 (1996)	Aug. 1995
807	Carlson, D. E., and D. A. Tortorelli	On hyperelasticity with internal constraints—*Journal of Elasticity* **42**, 91–98 (1966)	Aug. 1995

List of Recent TAM Reports (cont'd)

No.	Authors	Title	Date
808	Sayre, T. L., and D. N. Riahi	Oscillatory instabilities of the liquid and mushy layers during solidification of alloys under rotational constraint—*Acta Mechanica*, in press (1996)	Sept. 1995
809	Xin, Y.-B., and K. J. Hsia	Simulation of the brittle–ductile transition in silicon single crystals using dislocation mechanics	Oct. 1995
810	Ulysse, P., and R. E. Johnson	A plane-strain upper-bound analysis of unsymmetrical single-hole and multi-hole extrusion processes	Oct. 1995
811	Fried, E.	Continua described by a microstructural field—*Zeitschrift für angewandte Mathematik und Physik*, **47**, 168–175 (1996)	Nov. 1995
812	Mittal, R., and S. Balachandar	Autogeneration of three-dimensional vortical structures in the near wake of a circular cylinder	Nov. 1995
813	Segev, R., E. Fried, and G. de Botton	Force theory for multiphase bodies—*Journal of Geometry and Physics*, in press (1996)	Dec. 1995
814	Weaver, R. L.	The effect of an undamped finite-degree-of-freedom "fuzzy" substructure: Numerical solutions and theoretical discussion—*Journal of the Acoustical Society of America* **100**, 3159–3164 (1996)	Jan. 1996
815	Haber, R. B., C. S. Jog, and M. P. Bendsøe	A new approach to variable-topology shape design using a constraint on perimeter—*Structural Optimization* **11**, 1–12 (1996)	Feb. 1996
816	Xu, Z.-Q., and K. J. Hsia	A numerical solution of a surface crack under cyclic hydraulic pressure loading	Mar. 1996
817	Adrian, R. J.	Bibliography of particle velocimetry using imaging methods: 1917–1995—*Produced and distributed in cooperation with TSI, Inc., St. Paul, Minn.*	Mar. 1996
818	Fried, E., and G. Grach	An order-parameter based theory as a regularization of a sharp-interface theory for solid–solid phase transitions—*Archive for Rational Mechanics and Analysis*, in press (1996)	Mar. 1996
819	Vonderwell, M. P., and D. N. Riahi	Resonant instability mode triads in the compressible boundary-layer flow over a swept wing—*Physics of Fluids*, in press (1996)	Mar. 1996
820	Short, M., and D. S. Stewart	Low-frequency two-dimensional linear instability of plane detonation—*Journal of Fluid Mechanics*, in press (1997)	Mar. 1996
821	Casagranda, A., and P. Sofronis	On the scaling laws for the consolidation of nanocrystalline powder compacts—Proceedings of the IUTAM Symposium on the Mechanics of Granular and Porous Materials (1996)	Apr. 1996
822	Xu, S., and D. S. Stewart	Deflagration-to-detonation transition in porous energetic materials: A comparative model study—*Journal of Fluid Mechanics*, in press (1997)	Apr. 1996
823	Weaver, R. L.	Mean and mean-square responses of a prototypical master/fuzzy structure—*Journal of the Acoustical Society of America*, in press (1996)	Apr. 1996
824	Fried, E.	Correspondence between a phase-field theory and a sharp-interface theory for crystal growth—*Continuum Mechanics and Thermodynamics*, in press (1997)	Apr. 1996
825	Students in TAM 293–294	Thirty-third student symposium on engineering mechanics, J. W. Phillips, coordinator: Selected senior projects by W. J. Fortino II, A. A. Mordock, and M. R. Sawicki	May 1995
826	Riahi, D. N.	Effects of roughness on nonlinear stationary vortices in rotating disk flows—*Mathematical and Computer Modeling*, in press (1996)	June 1996
827	Riahi, D. N.	Nonlinear instabilities of shear flows over rough walls	June 1996
828	Weaver, R. L.	Multiple scattering theory for a plate with sprung masses: Mean and mean-square responses	July 1996
829	Moser, R. D., M. M. Rogers, and D. W. Ewing	Self-similarity of time-evolving plane wakes	July 1996
830	Lufrano, J. M., and P. Sofronis	Enhanced hydrogen concentrations ahead of rounded notches and cracks—Competition between plastic strain and hydrostatic constraint	July 1996

List of Recent TAM Reports (cont'd)

No.	Authors	Title	Date
831	Riahi, D. N.	Effects of surface corrugation on primary instability modes in wall-bounded shear flows	Aug. 1996
832	Bechel, V. T., and N. R. Sottos	Measuring debond length in the fiber pushout test—Proceedings of the ASME Mechanics and Materials Conference (1996)	Aug. 1996
833	Riahi, D. N.	Effect of centrifugal and Coriolis forces on chimney convection during alloy solidification—*Journal of Crystal Growth*, in press (1997)	Sept. 1996
834	Cermelli, P., and E. Fried	The influence of inertia on configurational forces in a deformable solid—*Proceedings of the Royal Society of London A*, in press (1996)	Oct. 1996
835	Riahi, D. N.	On the stability of shear flows with combined temporal and spatial imperfections	Oct. 1996
836	Carranza, F. L., B. Fang, and R. B. Haber	An adaptive space–time finite element model for oxidation-driven fracture	Nov. 1996
837	Carranza, F. L., B. Fang, and R. B. Haber	A moving cohesive interface model for fracture in creeping materials	Nov. 1996
838	Balachandar, S., R. Mittal, and F. M. Najjar	Properties of the mean wake recirculation region in two-dimensional bluff body wakes	Dec. 1996
839	Ti, B. W., W. D. O'Brien, Jr., and J. G. Harris	Measurements of coupled Rayleigh wave propagation in an elastic plate	Dec. 1996
840	Phillips, W. R. C.	On finite-amplitude rotational waves in viscous shear flows	Jan. 1997
841	Riahi, D. N.	Direct resonance analysis and modeling for a turbulent boundary layer over a corrugated surface	Jan. 1997
842	Liu, Z. C., R. J. Adrian, C. D. Meinhart, and W. Lai	Structure of a turbulent boundary layer using a stereoscopic, large format video-PIV	Jan. 1997
843	Fang, B., F. L. Carranza, and R. B. Haber	An adaptive discontinuous Galerkin methods for viscoplastic analysis	Jan. 1997
844	Xu, S., T. D. Aslam, and D. S. Stewart	High-resolution numerical simulation of ideal and non-ideal compressible reacting flows with embedded internal boundaries	Jan. 1997
845	Zhou, J., C. D. Meinhart, S. Balachandar, and R. J. Adrian	Formation of coherent hairpin packets in wall turbulence	Feb. 1997
846	Lufrano, J. M., P. Sofronis, and H. K. Birnbaum	Elastoplastically accommodated hydride formation and embrittlement	Feb. 1997
847	Keane, R. D., N. Fujisawa, and R. J. Adrian	Unsteady non-penetrative thermal convection from non-uniform surfaces	Feb. 1997
848	Aref, H., and M. Brøns	On stagnation points and streamline topology in vortex flows	Mar. 1997
849	Asghar, S., T. Hayat, and J. G. Harris	Diffraction by a slit in an infinite porous barrier	Mar. 1997
850	Shawki, T. G., H. Aref, and J. W. Phillips	Mechanics on the Web—Proceedings of the International Conference on Engineering Education (Aug. 1997, Chicago)	Apr. 1997
851	Stewart, D. S., and J. Yao	The normal detonation shock velocity–curvature relationship for materials with non-ideal equation of state and multiple turning points	Apr. 1997
852	Fried, E., A. Q. Shen, and S. T. Thoroddsen	Traveling waves, standing waves, and cellular patterns in a steadily forced granular medium	Apr. 1997
853	Boyland, P. L., H. Aref, and M. A. Stremler	Topological fluid mechanics of stirring	Apr. 1997